Republic of Iraq

Ministry of Higher Education

and Scientific Research

University of Babylon

College of Education for Pure Sciences

Department of Physics

Enhancement of Some Physical Characteristics of PS/SiO_2- $SrTiO_3$ for Environmental Applications

A Thesis

Submitted to the Council of the College of Education for Pure Sciences, University of Babylon in Partial Fulfillment of Requirements for the Degree of Master in Education / Physics

By

Arshad Fadhil Kadhim Matrud

B.Sc. of Science in Physics

University of Babylon/Department of Physics (2011)

Supervised by

Prof. Dr. Ahmed Hashim Mohaisen

2023 A.D **1444 A.H**

بِسْمِ اللَّهِ الرَّحْمَنِ الرَّحِيمِ

﴿وَقُل رَّبِّ أَدْخِلْنِي مُدْخَلَ صِدْقٍ
وَأَخْرِجْنِي مُخْرَجَ صِدْقٍ وَاجْعَل لِّي
مِن لَّدُنكَ سُلْطَانًا نَّصِيرًا﴾

صدق الله العلي العظيم

(سورة الاسراء - الاية ﴿٨٠﴾)

Dedication

To the Great Prophet of Good the Seal of Prophets "**Mohammed**".

To my Sir Amir of the Faithful, **"Imam Ali**".

To the eye that dreams of seeing me successful in the fields of life, **my father**.

To the one who filled me with her tenderness and compassion, and God helped me with approval with her supplication until she came out of darkness into light, **my mother**.

To the secret of my happiness, **my wife** and **my children.**

To my close **friends**, who have supported me all the way since the beginning of my studies.

To all **my teachers** who taught me to come to this stage of learning.

To everyone who supports me and stays beside me in my Life.

Arshad

Acknowledgement

In the name of Allah, the most merciful the most compassionate all praise be to Allah the lord of the worlds and prayers and peace be upon Mohamed his servant and messenger and to his good and pure household.

First and foremost, I thank the Almighty **Allah** for helping and giving me the ability to complete this thesis. Our thanks go to Prophet **Mohammed** and **AhlulBayt** (blessings of Allah be upon them all).

As I finish my thesis, I cannot but extend my sincere thanks and great gratitude to my dear supervisor Dr. **Ahmed Hashim** for his distinguished efforts, valuable advice and continuous direction to overcome all the difficulties that I faced throughout the period of work in order to make this thesis successful. For him my sincere appreciation and respect.

Finally, I would also like to thank all my friends and colleagues during the study in college of Education for Pure Sciences at Babylon University.

Arshad

SUMMARY

The nanocomposites of Polystyrene /Silica -Strontium titanate (PS/SiO_2-$SrTiO_3$) are prepared by casting solution method with various concentrations of SiO_2 and $SrTiO_3$ nanoparticles for the study of the structure, optical, and electrical properties of nanocomposites for used the antibacterial activity and gamma-ray radiation applications.

The structural properties are examined by the optical microscope (OM), scanning electron microscope (SEM), and Fourier Transforms Infrared Spectroscopy (FTIR), the optical microscope (OM) revealed a homogenous distribution of nanoparticles in the polymeric matrix and the formation of network routes as the concentrations of SiO_2 and $SrTiO_3$ NPs increased. The SEM images showed a homogeneous and good distribution in the surface morphology. The results of the FTIR measurements indicate that there is a physical interaction between the polymer (PS) and NPs (SiO_2 - $SrTiO_3$).

While results of optical properties for (PS/SiO_2- $SrTiO_3$) nanocomposites indicated the absorbance of (PS/SiO_2-$SrTiO_3$) nanocomposite increases as SiO_2-$SrTiO_3$ nanoparticle concentrations increase as both energy gap and transmittance decrease. When the SiO_2-$SrTiO_3$ nanoparticle ratios increase, the absorption and extinction coefficients, dielectric constant, real and imaginary parts of dielectric constant, optical conductivity, and refractive index are increased.

The results of the electrical properties of nanocomposites showed the dielectric loss for nanocomposites and dielectric constant are decreased with increasing frequency at the same time, while the A.C electrical conductivity increases. If the SiO_2-$SrTiO_3$ nanoparticle increase, the A.C electrical conductivity, dielectric constant, and dielectric loss of PS are increasing. The antibacterial application results of PS/SiO_2-$SrTiO_3$ nanocomposites showed that the inhibition zone for (E. coli) and (S. aureus) increases by an increase in the concentrations of SiO_2 -$SrTiO_3$ NPs. The results of applications of gamma-ray radiation showed when the SiO_2-$SrTiO_3$ NPs contents increase, the linear attenuation coefficients for gamma-ray radiation increase.

Contents

List of Figures

List of Tables

List of Abbreviations

	Physical Meanings
A.C	Alternating current
C.B	Conductive Band
E. coli	Escherichia coli bacteria
FTIR	Fourier Transform Infrared Radiation
NPs	Nanoparticles
OM	Optical Microscope
PS	Poly styrene
S. aureus	Staphylococcus aureus bacteria
SEM	Scanning Electron Microscope
SiO_2	Silica
$SrTiO_3$	Strontium titanate
UV	Ultraviolet
V.B	Valence Band

List of Symbols

Symbol	Physical Meaning
A	Absorbance
B	Constant Depended on Type of Material
C	Capacitance
c	Velocity of light
C_o	Vacuum Capacitor
C_p	Parallel Capacitance
D	Dispersion Factor
E_g	Energy Gap
E_g^{opt}	Optical Energy gap
E_{ph}	Phonon Energy
h	Plank constant
I	Instantaneous photon intensity
I_A	Absorbed Light Intensity
I_o	Incident Intensity of light
I_T	Intensity of transmittance ray
j	Imaginary number
K	Wave Vector

k	Extinction Coefficient
N	Number of particles counted over
N_O	Number of radiation particles counted over
N	Refractive index
R	Reflectance
r	Exponential constant
T	Transmittance
t	Thickness
V	Velocity of light
α	Absorption coefficient
$\mathcal{E}$	Complex dielectric constant
$\mathcal{E}_1$	Real dielectric constant
$\mathcal{E}_2$	Imaginary dielectric constant
$\mathcal{E}^*$	Complex permittivity
$\mathcal{E}_o$	Vacuum permittivity
$\mathcal{E}'$	Dielectric constant
$\mathcal{E}''$	Dielectric loss
ω	Angular frequency
$\sigma_{A.C}$	Alternating Conductivity

σ_{opt}	Optical conductivity
ν	Frequency
λ	Wavelength

1.1 Introduction

Researchers in science and technology have been interested in polymeric materials for their numerous uses. This is primarily caused by the materials' low weight, excellent mechanical strength, and optical qualities, which make them multipurpose materials. In light of its use in electronic and optical devices, research on the polymer's electrical and optical characteristics has recently garnered much attention [1].

To better understand the nature of the charge transport that occurs in these materials, electrical properties are one of the most practical and sensitive ways to study the physical mechanisms that determine this prop-polymer structure. In contrast, optical properties focus on improving reflection, antireflection, interface, and polarization properties [2].

Polymers are used as insulators because of their high resistivity and dielectric characteristics in a variety of products, such as printed circuit boards, corrosion-resistant electronics, and cable wrapping materials. Electrical gadgets employ polymer-based insulators to separate conductors without allowing current to flow through them. Numerous benefits exist for polymers, including low cost, simple production, adaptability, superior mechanical qualities, and great strength. It is employed in the nanolithography procedure utilized in the microelectronic manufacturing sector.

Polymeric nanocomposites, a type of material that has generated a lot of interest recently, are made up of organic polymers with inorganic nanoparticles. Applications for nanocomposites in microelectronic packaging, healthcare, cars, medication save , injection-molded goods, sensors, membranes, aerospace packaging materials, coatings, fire-retardant, adhesives, consumer goods… etc are extremely promising [3].

1.2 Polymer structure

The process of continuous connections to a chain or network structure of one or more molecules is known as polymerization. These huge molecules are categorized as monomers, which are the fundamental constituents of all other molecules [4] . Each molecule is composed of a large number of atoms bound together by covalent chemical bonds. The forces that draw molecules in polymers together vary on the kind of polymer. Because polymers are made up of enormous, coupled molecules that are difficult to manage, only a few crystal connections can be observed in polymers at low temperatures. A linear chain of molecules can only assemble itself in specific locations in an orderly manner. Polymers have crystalline and non-crystalline areas in their solid form [5]. According to their chemical compositions, polymers are divided into three primary types (linear, branched, and cross-linking Polymers), as shown in the Figure (1.1).

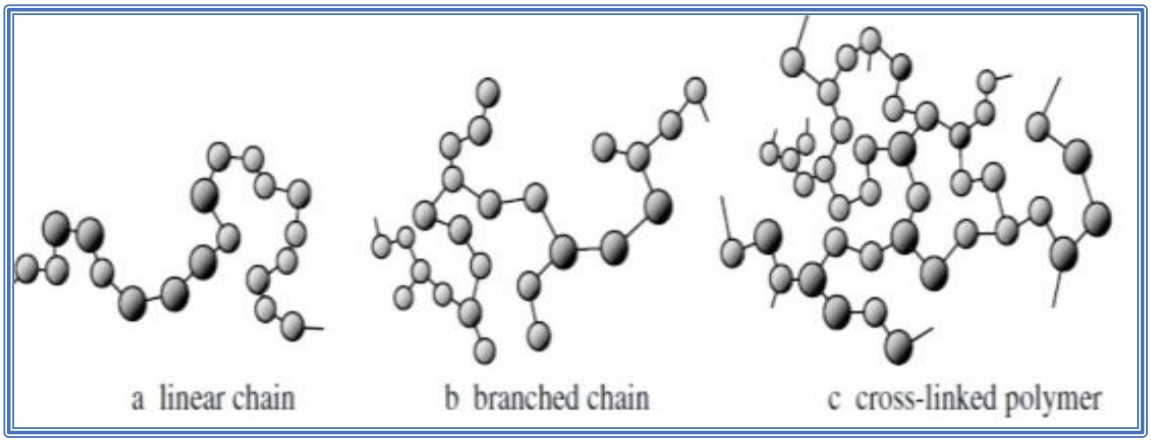

Figure (1.1): Constructivism Authority for a- Linear polymer, b- Branched polymer , c- Cross linked polymer [6].

Linear polymers these polymers have a linear structure and are generally thermoplastic polymers. The basic structure of these polymers is a single molecular chain of a certain length connected to each other in a linear form. They are soluble in solvents except for materials with extremely high molecular weight [7]. In the case of branching polymers, some branches form the primary polymer chain. Branching can change the physical

characteristics of a polymer, such as its solubility in solvents, softening point, and thermoplastic qualities. The last type is crosslinked polymers. These polymers have a three-dimensional network structure in which chemical linkages are intricately entangled [8].

1.2.1 Classification of polymers based on source

Polymers may be divided into two types [9]:

a. Natural polymer: It generally consists of proteins, carbohydrates, cellulose and rubber found in plants and animals, which primarily serve as structural support.

b. Synthetic polymer: Which constitutes the great majority of industrially necessary polymers including rubber, plastics, and synthetic leather, is created from straightforward chemical components. Other qualities offered by synthetic polymers include thermal stability, mechanical, and physical characteristics.

1.2.2 Classification of polymers based on thermal response

The following three types of polymers can be categorized based on how temperature affects them:

a. Thermoplastic Polymers: When the temperature rises, the molecules in thermoplastic polymers become elastic and sticky because they are held together by relatively weak intermolecular interactions (Vander - Waals forces), and when the temperature falls, they revert to their former condition. As with polyvinyl alcohol, polyethylene, polypropylene, and polystyrene, these molecules move across one another when heated [10], as shown in the Figure (1.2.a).

b. Elastomers Polymers: Elastomers are a type of network polymer that is weakly cross-linked and may be reversibly expanded to extraordinary lengths. When not under stress, their molecules are incredibly tightly and randomly coiled before expanding. Stretching polymers causes them to bend.

As a result, the chains are less random, which lowers the material's entropy. This entropy drop is caused by the retroactive force that has been seen. Cross-links prohibit molecules from passing one another when a material is expanded. As the rubbers cool, they get glassy or crystal transparent (partially). They don't flow when heated because of cross-links in the conventional sense [11], as seen in the Figure (1.2.b).

c. Thermosetting Polymers: When heated, a type of synthetic polymer known as thermosetting polymer undergoes chemical processes to generate a three-dimensional networked structure. This procedure produces a material that is insoluble and infusible; these properties are a direct outcome of the 3D network composed of covalent bonds. Because of this, thermosets cannot be reformed or remolded using heat or solvents as thermoplastics can. Thermosets include some kinds of crucial polymers for technology [12], as seen in the Figure (1.2.c).

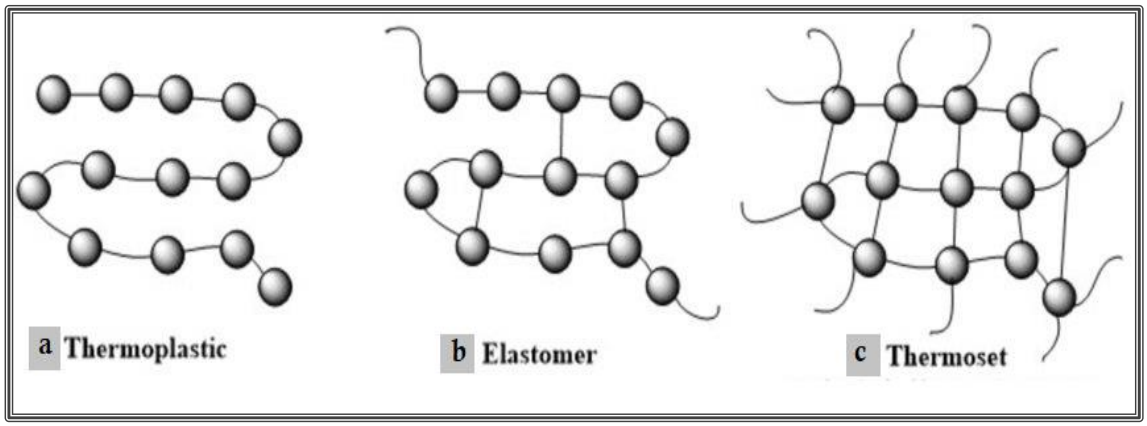

Figure (1.2): Schematic exemplification of a-Thermoplastic polymer, b-Elastic polymer, c- Thermoset polymer [13].

1.2.3 Classification of polymers based on homogeneity

Polymers are classified based on the homogeneity of the repeater units to:

a. Homo polymers: Polymers made from a single monomer species called the homo polymer , example for this is polyvinyl chloride(PVC)(monomer is vinyl chloride) [14].

b. Copolymers: Copolymers are made up of two units of duplicating units of different monomers. It is classified as random, alternative, block, and graft copolymers. An example of this is polyethene-vinyl acetate (PEVA) [15].

c. Composite polymers: It is The process of modifying the characteristics of homogenous polymers by including new materials and formulas [16].

1.3 Nanocomposites and some Applications

Generally speaking, nanocomposites outperform traditional composites in a variety of ways, including by enhancing the electrical, optical, and thermal properties, among others [17]. In addition to being light in both weight and size, a nanometer (nm) is one billionth of a meter. As a result, nanomaterials are substances whose smallest unit has a size between (1-100) nanometers [18]. Their powers are so promising that they might be employed in a variety of applications ranging from packaging to healthcare. These high-performance materials have exceptional property combinations and unique design options. Materials may show new properties, such as electrical conductivity, insulating properties, elasticity, improved strength, a different colour, and enhanced reactivity, with just a reduction in size and no alteration to the material itself [19]. However, polymer nanocomposites are at the forefront of applications due to their more advanced stage of research [20]. Additionally, nanomaterial-based composites can offer a variety of multifunctional qualities, including stability thermal, electronic qualities, field emission, optical quality, increased material durability, impact resistance, absorb energy and others [21].

1.4 Poly styrene (PS)

Polystyrene is a versatile polymer with the following properties transparency, ease of coloring and processing, and cheap cost. PS is a transparent stiff polymer that is resistant to a wide range of chemicals. PS has excellent flow properties and is hence very straightforward to process. It is valuable in optical and insulation applications due to its outstanding optical qualities, which include a high refractive index and strong dielectric properties. Packaging, housewares, toys, electronics, appliances, furniture, and building and construction insulation are among the applications of polystyrene [22]. PS is one of the greatest polymers, Its properties may be altered in a variety of ways, including physical mixing with other materials and copolymerization [23]. Because PS is amorphous, it lacks a clear melting point. This is seen by the material gradually deteriorating across a wide temperature range. While PS has a low intrinsic fire resistance and burns easily, starting flames long after the ignition source has been removed, polystyrenes respond well to high-energy radiation. PS is a superb insulator with high dielectric resistance, moderate stiffness, and a low loss factor even in wet conditions [24]. Figure (1.3) shows the chemical structure of polystyrene [25] , and table (1.1) shows some of the physical properties of polystyrene (PS) [26] .

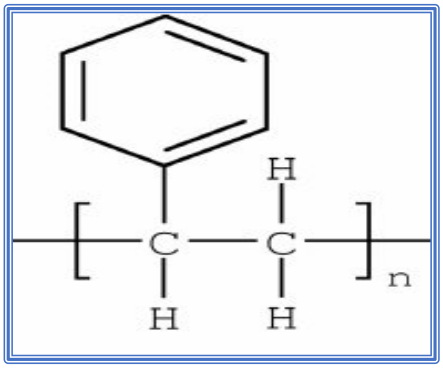

Figure (1.3). Chemical structure of PS [27].

Table (1.1): The physical properties of (PS) [28].

Parameters	PS
Chemical formula	$(C_8H_8)_n$
Density	(1.04 - 1.09) g/cm^3
Refractive index	1.59-1.60
Glass transition degree (Tg)	100 ^oC
Melting point (T_m)	240 ^oC
Tensile strength	(46–60) MPa

1.5 Silica (SiO_2) Nanoparticles and its Properties

Silica or Silicon dioxide is a silicon oxide with the chemical formula (SiO_2). Silica nanoparticles (SiO_2) are an intriguing material because of its thermal and chemical stability, low toxicity, ability to be functionalized with a range of chemicals and polymers, biocompatibility, physiological degradability, low cost, and so on. Nano-silica may also be widely used in a variety of different environmental protection sectors, such as batteries, paints, cosmetics, glass, steel, chemical fibers, plexiglass, and many more. Polymers containing silica nanoparticles offer much higher strength, hardness, wear, and aging resistance [28]. The addition of (10nm) SiO_2 to PS increased its hardness and thermal stability [29]. Table (1.2) show some properties of SiO_2 [30].

Table (1.2) : Some properties of SiO_2 [30].

Chemical formula	**SiO_2**
Density	2.4 g/cm^3
Color	White
Specific surface area (BET)	180 m^2 /g

1.6 Strontium titanate ($SrTiO_3$) Nanoparticles and its Properties

Strontium titanate ($SrTiO_3$) nanoparticles are incipient ferroelectric materials because their ferroelectricity is preserved at low temperatures by quantum functions. They are recognized for their ability to serve as high-temperature resistive oxygen sensors and transition to non-ferroelectric characteristics at lower temperatures**.** $SrTiO_3$ has a high dielectric constant. Their unique properties, which include high breakdown strength, low leakage current density, low dielectric loss, tuneability, and high dielectric constant [31]. $SrTiO_3$ has potential use in environmental cleaning and renewable energy generation [32]. has improved corrosion resistance, and other advantages Due to its excellent properties, $SrTiO_3$ may be employed in oxygen sensors, organic thin film transistors, dye-sensitized solar cells (DSSCs), and other applications [33]. Table (1.3) shows some properties of $SrTiO_3$ [34].

Table (1.3): Some properties of $SrTiO_3$ [34].

Chemical formula	**$SrTiO_3$**
Melting point	2080 °C
Refractive index	2.31-2.38
Density	5.2 g/cm³
Color	Gray/White off

1.7 Literature Review

In (2015), M. Awad, *et. al* [35]**,** studied the antibacterial activity of a silver/polystyrene nanocomposite against both bacteria (positive and negative) grams. This suggests that the nanocomposite might be used in pharmaceutical, biological, and industrial domains, such as bandages, wound dressings, and dental instruments. Furthermore, the uses include food and water storage, as well as wastewater treatment.

In (2015), M. Kadhim [36], studied the nanocomposite (PS/Ti) in a casting manner with the addition of different weight ratios of nano titanium. With increasing Ti weight ratios, the extinction coefficient and absorption coefficient rise, while the energy gap of the indirect allowed and forbidden transition decreases.

In (2016), M. Al-Saleh and S. Abdul Jawad [37]**,** prepared the graphene nanoplatelet–polystyrene (GNP–PS) nanocomposites using melt-mixing. Used the microstructure, direct current electrical percolation behaviour, and dielectric properties for studied the frequency. The electrical percolation curve demonstrated a constant change from insulation to conduct. They

found that the dielectric constant and loss factor of 180 and 0.11, respectively, with 15 wt.% GNP loading at a frequency greater than 104 Hz, revealing exceptional storing capacities at high frequencies.

In (2016), H. Shanshool, *et. al* [38]**,** they prepared a composed polymer matrix (PMMA-PVDF-PVA-PS), while the filler is of ZnO nanoparticles in various concentrations. transmittance is low in the UV regions, as seen in UV-visible transmittance spectra, which are inversely proportional to ZnO nanoparticle concentration. As the weight % of ZnO nanoparticles in nanocomposites increased, the energy gap values decreased for all samples.

In (2017), X. Zhang, *et. al* [39], studied the $SrTiO_3$/epoxy nanocomposites created by adding $SrTiO_3$ nanoparticles of various weight fractions to the epoxy resin host, the shape of the nanoparticles and composites, and their electrical and thermal conductivity qualities. As the weight fractions increased, the dielectric constant also and the frequency dropped. The tests revealed substantial improvements in the composites' thermal and electrical characteristics.

In (2017), S. Moharana, *et. al* [40]**,** used solution casting techniques to prepare the three-phase PS-BFO-GNP nanocomposite films with GNP acting as a conductive filler. It is discovered that adding GNP to the matrix of PS-BFO nanocomposites may significantly increase their dielectric constant. The improvement in dielectric and ferroelectric characteristics supports the prospect of end-use usability as a new class of polymer-based materials for electronic device applications.

In (2018), D. Hassan and A. Hashim [41]**,** prepared of (polystyrene-copper oxide) nanocomposites and studied the structural and optical characteristics for biological applications. They found that the optical conductivity, absorbance, refractive index, absorption coefficient, extinction coefficient, real dielectric constant and imaginary dielectric constant of polystyrene increase when CuO nanoparticle concentrations rise, whereas transmittance

and energy band gap decrease. The attenuation coefficients for gamma radiation sources (Cs-137) rise as the quantities of CuO nanoparticles increase.

In (2018), G. Soni *et. al* [42]**,** they fabricated PMMA/SiO_2 nanocomposite using the solution casting method and investigated the effect of SiO_2 nanoparticle (NP) loading on the optical and mechanical properties of the composite thin film. The SEM images show that nanocomposite thin films have a smoother and uniform morphology. It is observed that the optical bandgap decreases with an increase in the SiO_2 NP concentration.

In (2019), M. Habeeb, *et. al* [43] , studied the dielectric characteristics of (PS-Cr_2O_3). They demonstrated that the AC electrical conductivity, dielectric loss, and dielectric constant of (PS-Cr_2O_3) nanocomposites increase when ($ZnCoFe_2O_4$) nanoparticle concentrations increase. As frequency increases, electrical conductivity increases while the dielectric loss and dielectric constant decrease.

In (2020), R. Hashim, *et. al* [44]**,** used the casting process to create a polystyrene-poly (methyl) methacrylate (PS-PMMA) mix and its nanocomposite with different ZnO/Fe_2O_3 ratios. They found that the absorption increases of UV rays by increasing the ZnO/Fe_2O_3 ratios. The energy gap for both indirect transitions (allowed and forbidden) decreased by increasing the ZnO/Fe_2O_3 ratios.

In (2020), L. Weng, *et. al* [45]**,** studied the PVDF/Ag@SiO_2 nanocomposite's high dielectric properties. This resulted in the Ag@SiO_2 having a rise in dielectric constant and low electrical conductivity dependent on frequency. They can get Ag@SiO_2/PVDF composites of frequency constant in electrical conductivity by the concentration of nanoparticles. Ag@SiO_2/PVDF composite materials may be used as material for energy storage.

In (2020), G. Soni, *et. al* [46], studied the impact of a mixture of ZnO and SiO_2 nanoparticles on the optical properties of a solution-cast composite thin film PMMA/ZnO/SiO_2, with a thickness of 50 µm, and discovered that the optical bandgap of the composite thin films decreases with increasing concentrations of zinc oxide and silica .

In (2021), B. Rabee and R. Haider [47], studied electrical properties of nanocomposite generated by adding (Ag) nanoparticles and the effect on the (SPO-PS-PMMA) blend. They found the A.C electrical conductivity increase with increasing the frequency of the electric field and increasing concentrations of the (Ag) nanoparticles, while the dielectric constant decreases with increasing frequency (from 100Hz to 3.E06Hz) and the dielectric constant decreases increases with increasing concentrations of the (Ag) nanoparticles..

In (2021), L. Gaabour [48]**,** studied the impact of adding titanium oxide nanoparticles (TiO_2) to a polymer mix of polystyrene (PS) and polyvinyl chloride (PVC) with a composition of 50/50 wt.%. Using new methods, the produced polymer nanocomposite films' structural, optical, and dielectric characteristics are examined. Refractive index, optical dielectric (constant and loss), and other optical characteristics including absorbance, reflection, bandgap energy, and others are examined. These findings demonstrated that interband between the valence and conduction bands are produced by TiO_2. Because of charge carrier accumulation and improved polymeric chain motion inside the polymeric matrix, adding TiO_2 to the PS/PVC increase the PS/PVC electrical conductivity.

In (2022), O. Fadil and A. Hashim [49]**,** they made nanostructures made of silicon dioxide, cerium dioxide, and poly-methyl methacrylate (PMMA). The CeO_2/SiO_2/PMMA nanostructures examined optical characteristics. The energy gap of PMMA is decreased with the increase of the CeO_2/SiO_2 NPs. The content of CeO_2/SiO_2 NPs increased, which increased the refractive

index, optical conductivity, and dielectric constants of PMMA. The results demonstrated that PMMA/CeO_2/SiO_2 nanostructures have good optical properties for use in the fields of optics and electronics.

In (2022) , M. Meteab , *et .al* [50]**,** studied the structural and dielectric characteristics of (PS-PC/Co_2O_3-SiC) nanocomposites. The FTIR measurements demonstrated that the polymer matrix and (Co_2O_3/SiC) NPs do not interact chemically. The dielectric characteristics are investigated at frequencies ranging from 100 Hz to 5×10^6 Hz. According to the results of the dielectric characteristics, the dielectric constant and dielectric loss of (PS-PC/Co_2O_3-SiC) nanocomposites as increased the concentration of (Co_2O_3/SiC) NPs increased. However, they decreased as the frequency increased; when the frequency and concentration of (Co_2O_3/SiC) NPs increased the A.C conductivity of (PS-PC/Co_2O_3-SiC) nanocomposite increased.

1.8 The Aim of the Study

- To prepare PS/SiO_2-$SrTiO_3$ new nanocomposites.

- To study the effect addition of SiO_2-$SrTiO_3$ NPs on the optical, structural, and dielectric properties of PS/SiO_2-$SrTiO_3$ nanocomposites.

- To study the antibacterial activity and gamma-ray radiation applications of PS/SiO_2-$SrTiO_3$ nanocomposites.

Chapter Two

The Theoretical Part

2.1 Introduction

This chapter provides an overview the part of theoretical of this study, including physical ideas, scientific clarifications, laws used to explain the study's conclusions, and relationships.

2.2 The Structural and Morphology properties

2.2.1 The Optical Microscope (OM) and Scanning Electron Microscope (SEM)

Optical microscopy (OM) is the oldest and has been in use for the past 200 years as a straightforward device with constrained functions. Additionally known as light microscopy. evaluates how well the nanoparticles are incorporated into the polymer with high uniformity [51]. Scanning electron microscope (SEM) is a versatile device frequently used to examine material surface characteristics. In a SEM, the material is bombarded with high-energy electrons, and the ejected electrons are subsequently examined. These released electrons offer information on the topography, morphology, crystallographic information, etc. of a material. Topography describes a sample's surface properties, including its texture, smoothness, and degree of roughness, whereas morphology describes a sample size and form [52].

2.2.2 Fourier Transform Infrared Spectroscopy (FTIR)

The preferred technique of infrared (IR) spectroscopy is Fourier transform infrared (FTIR). Where (IR) radiation passes through the sample, and IR radiation is absorbed for some, and some are reflected by the sample (transmitted). The resultant spectrum represents molecule absorption and transmission, forming the ample molecular fingerprint. Just as no two unique molecule structures create the same IR spectrum, no two unique molecular structures produce the same IR spectrum. As a result, IR spectroscopy may

be used for a variety of analyses. For nearly 70 years, IR spectroscopy has been a workhorse tool for materials investigation in the laboratory [53].

2.3 The Optical Properties

Many optical characteristics are studied and researched as a result of their uses in optics. The study of absorption is important for determining direct and indirect transitions [54].The study of optical characteristics is critical in determining the optical constants that may be used. Identifying the optical energy gap, as well as the other absorption and transmittance constants and coefficients, as well as the extinction coefficient and the real and imaginary dielectric coefficients [55].

2.3.1 Absorbance (A)

It can be defined as the proportion of the intensity of light absorbed (I_A) to the intensity of the incoming light, and the absorbance is a quantity that has no units. It results from the relationship described below [56].

$$A = I_A / I_o \quad \text{..... (2.1)}$$

2.3.2 Transmittance (T)

The transmitted intensity ratio (I_T) to the intensity of the rays of the incident on the material (I_o) is known as transmittance, as shown in the equation [57].

$$T = I_T / I_o \quad \text{..... (2.2)}$$

2.3.3 Reflection (R)

The reflectivity (R) can be defined as the proportion of the intensity of the radiation reflected from the film in a particular direction to the original intensity of the radiation incident on it. The value of the reflectivity can be

calculated using the law of energy conservation and knowledge of spectral absorption and permeability. In the following situation [58].

$$A+ R+T=1 \ldots\ldots\ldots\ldots\ldots\ldots\ldots \quad (2.3)$$

2.3.4 Fundamental Absorption Edge

The absorption edge is located at the visible part from the spectrum and is divided into three portions [59], as seen in the Figure (2.1) , which shows the absorption zones:

A) High absorption region: The first section is in the high absorption coefficient region, $\alpha > 10^4$ cm $^{-1}$.

B) Region exponential: In this part, where equals absorption coefficient is :

$1\ cm^{-1} < \alpha < 10^4\ cm^{-1}$.

C) Region absorption low: In this range of the absorption coefficients ($\alpha < 1$ cm $^{-1}$) the absorption coefficient is tiny [60] .

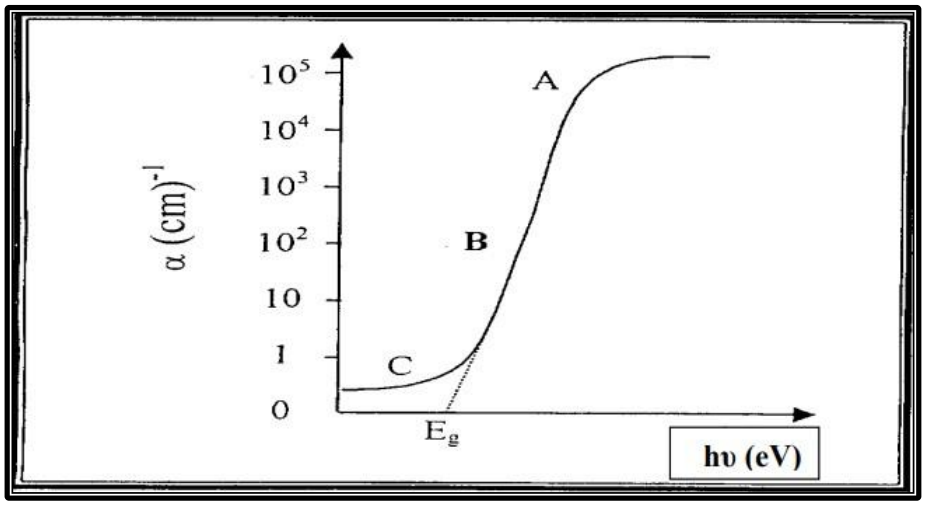

Figure (2.1): The absorption regions showing three different A, B and C [60].

2.3.5 The Electronic Transitions

Electronic transitions are divided into two categories [61]:

1. Direct Transition

Direct transition often happens between the valence band at the top part from him of and the conduction band at the bottom from him of at the same

wave vector (ΔK = 0) have momentum conservation. It has two types of direct transitions [62].

a) **Direct Allowed Transition**: Transition directly that happens between the top part of the valence band (V.B)and the part bottom of the conduction band (C.B), known as the allowed direct transition, takes place when the wave vector's change equals zero (ΔK= 0), Figure (2.2-a) shows that.

b) **Direct forbidden transitions**: That transition directly happens between both the valence band(V.B) near the top part of him and the conduction band(C.B) near the bottom part of him, as seen in the Figure (2.2-b). Where the formula following gives the absorption coefficient in this transition [63] :

$$\alpha h\upsilon = B\,(h\upsilon - E_g^{opt})^{r} \quad \ldots\ldots\ldots\ldots\ldots\ldots\ldots\ldots \quad (2.4)$$

where: E_g^{opt} : optical energy gap .

α: is the absorption coefficient.

B: constant depended on type of material.

υ: is the photon frequency.

h: constant known as Planck's constant.

r: constant of exponential, it depends on the transition and type for it.

r =1/2 for transitions are directly allowed.

r =3/2 for transitions are directly forbidden.

2. Indirect Transitions

In this transition type, the valence band's is not down the conductivity band's bottom. The electron does not go perpendicularly from (V.B) to (C.B). they are in various areas of (K) space (ΔK ≠ 0). This form of transition is made possible by a particle known as a "Phonon." Indirect transitions are classified into two categories [62]:

a) Allowed indirect transitions: Figure (2.2-c) shows that similar transitions indirectly happen between both (V.B) the valence band at the top part of him and (C.B) the conduction band at the bottom from him in a different region of (K-space).

b) Forbidden indirect transitions: This transition indirectly happens between both the valence band (V.B) near the top part of him and the conduction band (C.B) near the bottom of him, as indicated in the Figure (2.2-d). Phonon on absorption denotes the coefficient of transition absorption:

$$\alpha h\upsilon = B\left(h\upsilon - Eg^{opt} \pm E_{ph}\right)r \quad \ldots\ldots\ldots\ldots\ldots\ldots\ldots (2.5)$$

where: E_{ph}: Phonon energy: when phonon absorption, the energy is (-), and when phonon emission, the energy is (+).The transitions indirect allowed (r = 2)and for the transitions indirect forbidden (r = 3) [64].

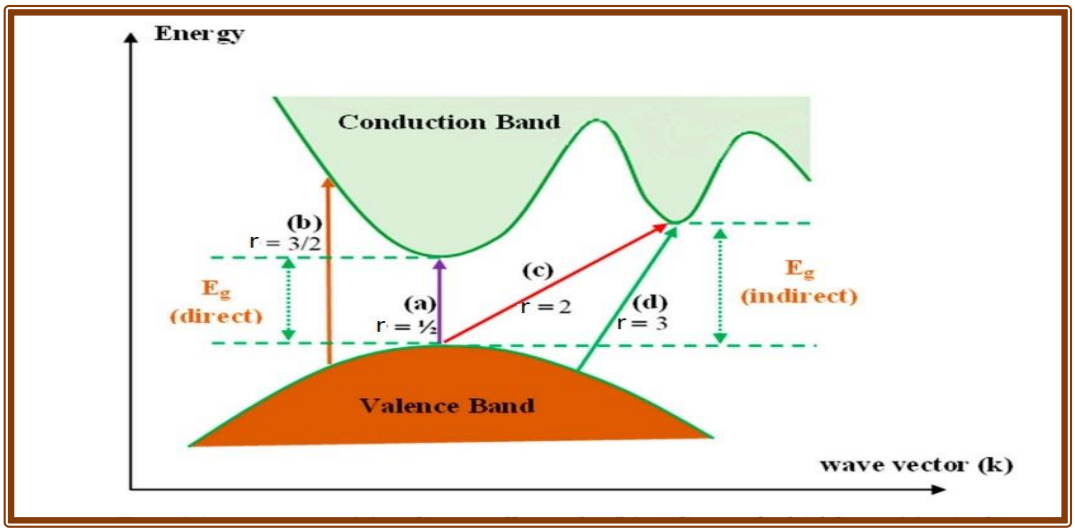

Figure. (2.2): The transition types [64].

(a) Transitions are directly allowed. **(b) Transitions are directly forbidden.**

(c) Transitions are indirectly allowed. **(d)Transitions are indirectly forbidden.**

2.3.6 Optical Constants

Numerous factors make the study of composite materials' optical constants interesting. All substances' optical characteristics depend on their

electronic band structure, atomic structure, and electrical properties [65]. There are several methods for determining the optical constants' absorption for each of the coefficients absorption and extinction, refractive index, dielectric constant and optical conductivity.

1. Absorption Coefficient (α)

The absorption coefficient (α) in the direction of a wave's spread in a medium is the gradual decrease in energy flow in an incident field. For polymer nanocomposites the optical absorption coefficient depends on photon energy for band structure determination and the type of electron transition [66]. Using the (Beer-Lambert) equation can be calculated the absorption coefficient (α), which is dependent on each of the transmittance (T)and the absorbance (A) [67].

$$I=I_o\, e^{-\alpha t} \quad \ldots\ldots\ldots\ldots\ldots\ldots\ldots\ldots\ldots\ldots\ldots (2.6)$$

(I) is instantaneous photon intensity while (I_o) is initial photon intensity, and (t) is the thickness.

$$\alpha t = 2.303 \log I/I_o \quad \ldots\ldots\ldots\ldots\ldots\ldots\ldots\ldots\ldots (2.7)$$

Where the absorption (A) here represents log I/Io, so the absorption coefficient is determined [67]:

$$\alpha = 2.303(A/t) \quad \ldots\ldots\ldots\ldots\ldots\ldots\ldots\ldots\ldots\ldots (2.8)$$

2. Extinction coefficient (k)

The imaginary fraction for the complex refractive index symbolizes here for the extinction coefficient. It is defined as the amount of electromagnetic radiation attenuation caused by electromagnetic rays interacting with particles in the thin film material [68]. It (k) can be computed using the equation [69]:

$$k = \alpha\lambda / 4\pi \quad \ldots\ldots\ldots\ldots\ldots\ldots\ldots\ldots\ldots\ldots (2.9)$$

where λ (cm) is the incident radiation's wavelength.

3.Refractive index (n)

The velocity of light in a vacuum to the velocity of light in a sample of a material, that ratio is known as the refraction index:

$$n = c / v \quad \text{(2.10)}$$

Where (v) the velocity of light in any material medium ,and (c) the velocity of light in a vacuum[70]. For the finding of the sample refractive index, they are taken into consideration the reflectance (R) and the extinction coefficient (k), the equation is used [71]:

$$n = \left[\frac{1+R}{1-R}\right] + \sqrt{\frac{4\times R}{(1-R)^2} - k^2} \quad \text{(2.11)}$$

4. Dielectric constant ($\mathcal{E}$)

One of the essential dielectric parameters, which plays a significant role in determining material properties, is the dielectric constant. It is related to the dipole moment, polarizability, etc. The dielectric constant may be determined using the equation Maxwell for electromagnetic radiation [72]:

$$\mathcal{E} = n^2 \quad \text{(2.12)}$$

Where the complex dielectric constant is described as ($\mathcal{E}$), and ($\mathcal{E}_1$) is the real part of the dielectric constant and ($i\mathcal{E}_2$) the imaginary part of the dielectric constant. The real dielectric constant, the imaginary dielectric constant, and dielectric constant can be found by equitations [72] :

$$\mathcal{E} = \mathcal{E}_1 - i\mathcal{E}_2 \quad \text{(2.13)}$$

$$\mathcal{E}_1 = n^2 - k^2 \quad \text{(2.14)}$$

$$\mathcal{E}_2 = 2nk \quad \text{(2.15)}$$

5. Optical Conductivity (σ_{opt})

The optical conductivity (σ_{opt}) results from the movement of charge carriers yielded by the alternating electric field of incoming electromagnetic waves, as shown in the following equation [73]:

$$\sigma_{opt} = \frac{\alpha n c}{4\pi} \quad \text{.....(2.16)}$$

2.4 Electrical Properties

Nanotechnologies are an enticing field of study that may significantly influence the creation of cutting-edge electrical and electronic goods. A few per cent of functional nanofillers are sufficient to drastically alter the electrical characteristics of polymers in nanocomposites [74]. Electrical energy storage is crucial for mobile electronics, fixed power systems, hybrid electric cars, and pulse power applications. Particularly, there is an increasing need for capacitors that can store a substantial quantity of energy and then release it very instantly. Over time, these applications need ever-increasing energy and power densities and high-rate capabilities [75].

2.4.1 The A.C electrical conductivity

As an external electric field polarizes the electrons surrounding component molecules or atoms, can be used dielectric materials to store electrical energy during charge separation. The complex permittivity ($\mathcal{E}^*$) of a material may be represented as [76]:

$$\mathcal{E}^* = \mathcal{E}_1 - j\,\mathcal{E}_2 \quad \text{.....(2.17)}$$

where $\mathcal{E}_1$ and $\mathcal{E}_2$ are the real and the imaginary part, respectively, and the imaginary number is ($j= \sqrt{-1}$). The real part is determined by [76]:

$$\mathcal{E}_1 = \mathcal{E}_o\,\mathcal{E}' \quad \text{.....(2.18)}$$

Where $\mathcal{E}_o$ is the permittivity of vacuum and $\mathcal{E}'$ is the permittivity relative of materials. The values of $\mathcal{E}_1$ and $\mathcal{E}_2$ dependent on the frequency of the applied electric field. The values of the $\mathcal{E}_1$ (or the dielectric constant $\mathcal{E}'$) refers to the material can store energy from an applied electric field [76]. he formula of the capacitance of a capacitor constructed of two parallel plates gives [77]:

$$C = \mathcal{E}' \mathcal{E}_o A/t \quad \text{……………………………….(2.19)}$$

Where ($\mathcal{E}$): the dielectric constant.

(t): the thickness for the samples. The formula for dielectric constant is [77]:

$$\mathcal{E}' = C_P / C_o \quad \text{……………………………….(2.20)}$$

Where: C_o is the vacuum capacitor and capacitance the parallel is C_P. The formula calculates dielectric loss ($\mathcal{E}''$) [78]:

$$\mathcal{E}'' = \mathcal{E}' D \quad \text{…………………………………..(2.21)}$$

The dispersion factor here is known as (D), which calculates the electrical energy lost in the samples due to the applied field being converted to thermal energy. Dissipated power in the insulator is demonstrated by alternative capacity as a function of the conductivity of the alternative by equation [79]:

$$\sigma_{A.C} = \omega \mathcal{E}_o \mathcal{E}'' \quad \text{……………..………………(2.22)}$$

Where ω is an angular frequency.

2.5 Anti-Bacterial Activity

The emergence of infectious illnesses and antibiotic-resistant bacterial species, in particular, represent a grave danger to global public health. Gram-positive and Gram-negative bacterial strains are generally believed to pose a significant threat to public health. Antibacterial agents are important to stop the growth of microorganisms and decrease their detrimental impact on people's lives. Inorganic antibacterial compounds such as metal oxides are antibacterial agents that very appear promising [80]. Due to their unusual physical, chemical, and biological characteristics in several domains, including medicine, nanoparticles have attracted considerable interest. It is simple to adjust the characteristics of nanoparticles by lowering or hanging their size [81]. Nanoparticles have the ability to solve this issue by providing a viable option to treat diverse illnesses, especially those caused by multidrug-resistant (MDR) bacteria. In general, the antibacterial effect of designed NPs involves the surface-binding of the NPs to the bacterium, the release of ions, and the subsequent development of severe oxidative stress. Therefore, it becomes very challenging for bacteria to evolve numerous simultaneous gene changes to resist NP-mediated therapies [82].

2.6 Gamma Ray Shielding

There are general radiation protection standards that vary depending on the distance and time. The type and quantity of shielding required are determined by the functioning of the radiation source, the exposure intensity, and the type of radiation [83]. Radiation shielding materials may be fabricated in two different methods. First, shielding materials are installed directly or on the surface of the wall. Second, these molecules encapsulate the radioactive source. For radiation shielding, any material with sufficient

thickness to absorb incident radiation to a reasonable degree should be used [84].

$$N=N_O \exp(-\mu t) \quad \text{.....(2.23)}$$

is a formula that describes the attenuation of radiation gamma, where the attenuation coefficient is (μ), (t) is the thickness of the specimen, N_O is the number of radiation particles calculated over time, and N is the number of particles calculated over [85].

Chapter Three

The Experimental Part

3.1 Introduction

This chapter describes the preparation procedure, instruments, and measurement methods. A basic description of the materials (PS/SiO_2-$SrTiO_3$) used in this study and measurement processes for structural, optical, and electrical properties for antibacterial activity applications, along with photos and schematics of some of the electrical circuits.

3.2 The Materials Used in this Work

3.2.1 Matrix Material

In this work, polymer matrix polystyrene is used in granular form and high purity (99.97%) and readily available in local marketplaces. PS is an amorphous polymer with many side groups. It is hard, stiff, and transparent at room temperature, and it is a thermoplastic substance that can be softened and deformed by heat, as shown in the Figure (3.1).

Figure (3.1): Polystyrene (PS).

3.2.2 Additive Nanomaterials

1. Silicon dioxide (SiO_2)

Silicon dioxide (SiO_2), or silica nanoparticles, is used extensively in biomedical research owing to its stability, low toxicity, and ability to be functionalized with various chemicals and polymers The silicon dioxide nanopowder (SiO_2, +98 %, 60 – 70 nm, amorphous) was obtained from (US

Research Nanomaterials, lnc). It appears in white powder, as seen in the Figure (3.2):

Figure (3.2): Silica dioxide nanoparticles.

2. Strontium titanate ($SrTiO_3$)

It is oxide strontium and titanium have the chemical ($SrTiO_3$). Strontium titanate has a low electric field and high dielectric constant. Strontium Titanate nanoparticles ($SrTiO_3$) is obtained as powder form and could be obtained from the (US Research Nanomaterials, Inc) company, with the value radius (100 nm) and the high purity (99.95 %), as shown in the Figure (3.3).

Figure (3.3): Strontium titanate ($SrTiO_3$) nanoparticles.

3.3 Preparation of (PS/SiO_2- $SrTiO_3$) Nanocomposites

The nanocomposite (PS/SiO_2- $SrTiO_3$) was prepared by casting method (1g) of the polystyrene (PS) is dissolved in (30) ml of chloroform alcohol, at room temperature and a magnetic stirrer is used to mix and thoroughly dissolve the substance. We'll add the nanoparticles (50%) from SiO_2 and (50%) $SrTiO_3$ to (PS) with contents (1.6, 3.2, 4.8, and 6.4) wt.%. The casting process, which involves placing the mixture in a template (Petri dish) with a (10 cm) diameter, allowing it to dry, and then gently extracting it from the template in order to do the required tests. Figure (3.4) shows a scheme of experimental work.

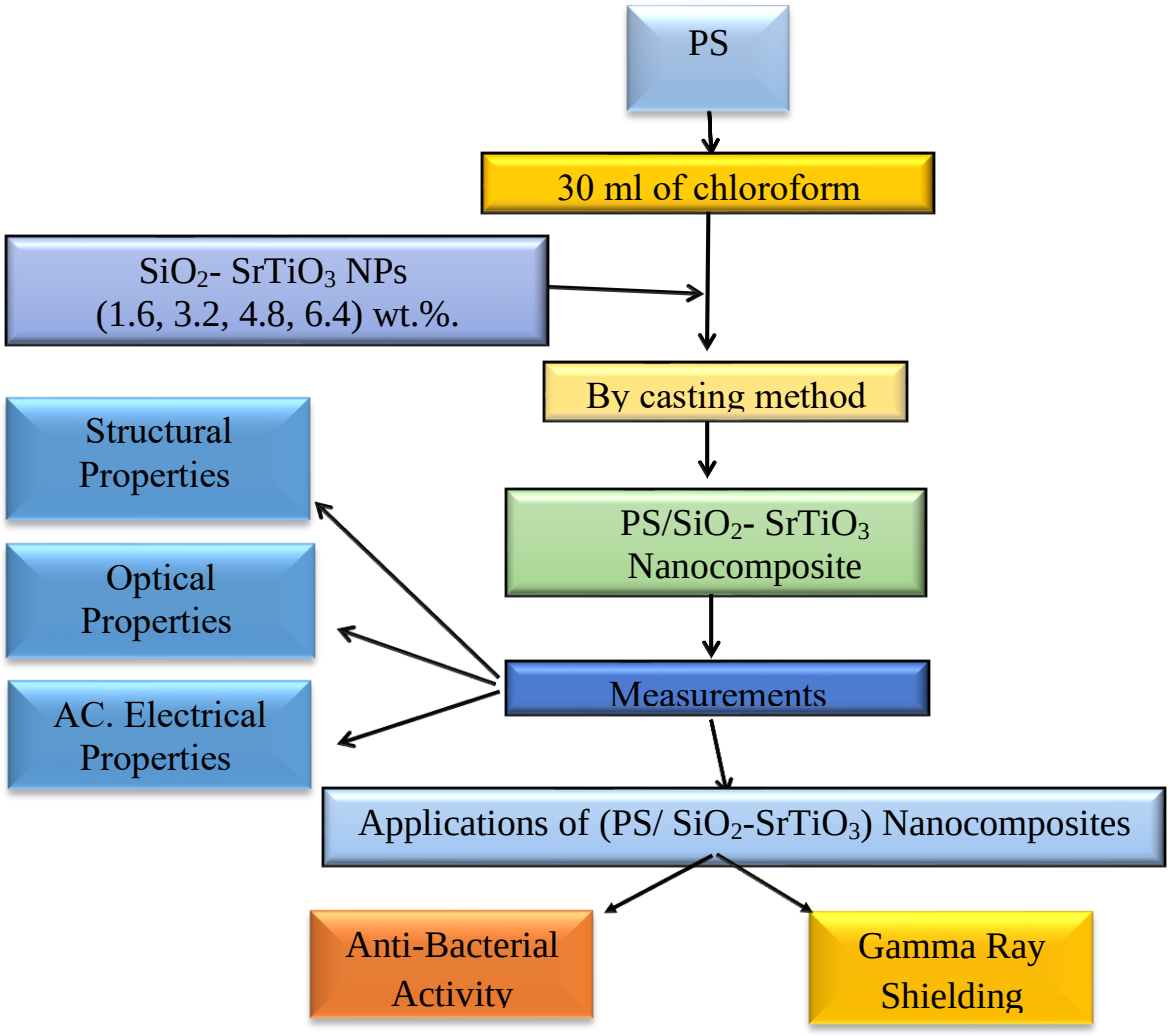

Figure (3.4): Scheme of Experimental work.

3.4 Measurements of Structural Properties

3.4.1 Optical Microscope (OM)

Samples (PS/SiO_2- $SrTiO_3$) are examined using an optical microscope (Olympus (Toup View) type (Nikon-73346)) with magnification (10X),in College of Education for Pure Sciences, Babylon University as shown in the Figure (3.5).

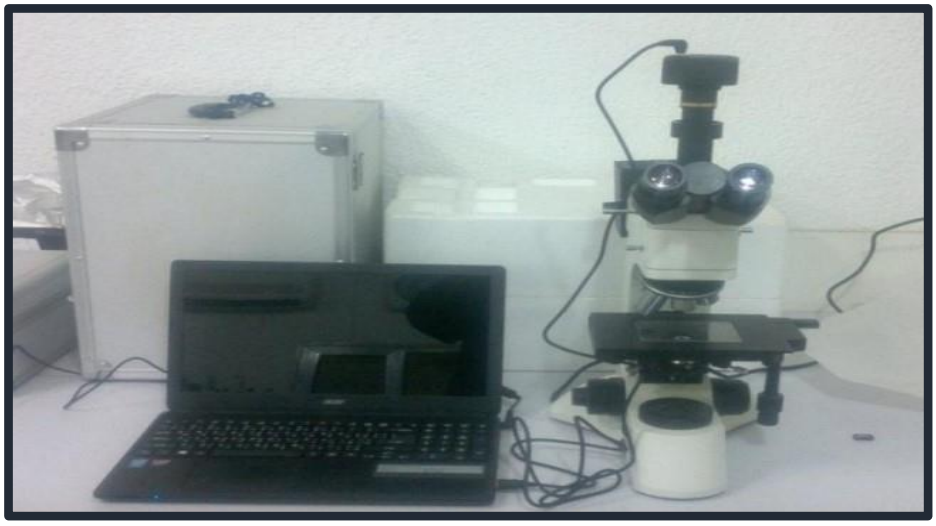

Figure (3.5): Optical Microscope.

3.4.2 Scanning Electron Microscope (SEM)

The surface morphology of all nanocomposites (PS/SiO_2- $SrTiO_3$) is analyzed using a scanning electron microscope. It produces black-and-white pictures of the sample's surface since it does not rely on light waves but on electronic emission, and it magnifies the image with a high degree of precision, around 10^9 times. At the Shahrud University of Technology, Iran, a scanning electron microscope (Zeiss, Sigma, German origin) is used for testing. Figure (3.6) is an image of the SEM device and a schematic representation of the usual SEM column.

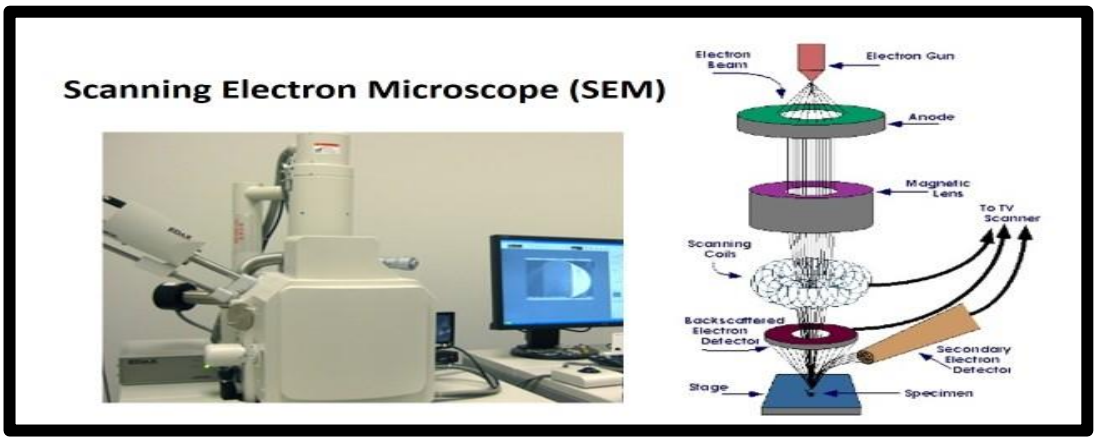

Figure (3.6): The SEM device [86].

3.4.3 Fourier Transform Infrared Spectroscopy (FTIR)

FTIR spectra of PS/SiO_2- $SrTiO_3$ by FTIR are recorded from made German Brucker Company from type vertex-70 Fourier transforms infrared spectrometer in the wavelength range (500-4000) cm^{-1}, in College of Education for Pure Sciences, Babylon University.

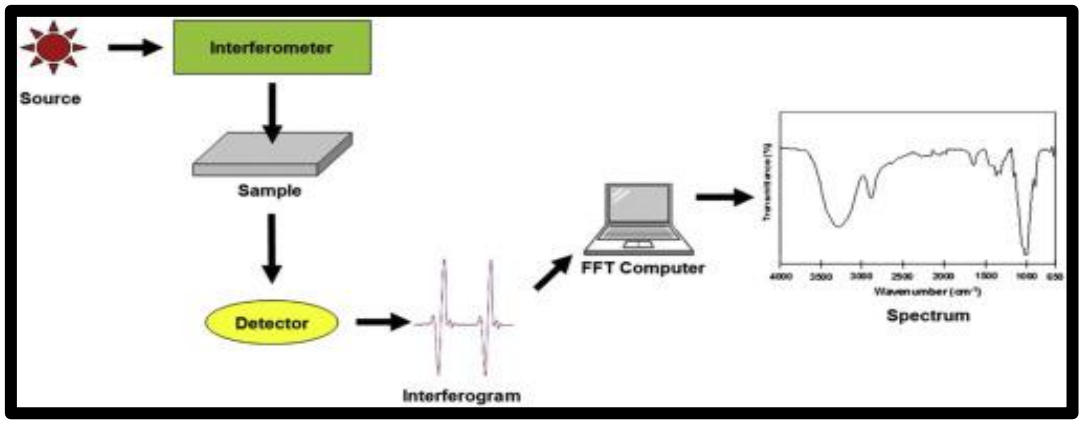

Figure (3.7): (FTIR) Fourier transform infrared spectroscopy device [87].

3.5 Optical properties measurements

Using a dual-beam spectrophotometer (Shimadzu, UV-1800A^{o}) located at Babylon University, the College of Education for Pure Sciences, the absorption, transmittance, and reflection are measured spectrum of nanocomposites (PS/SiO_2- $SrTiO_{3)}$ in the wavelength range (260-860) nm are recorded. These observations were conducted at room temperature.

3.6 Measurements of A.C Electrical Properties for Nanocomposites

The A.C electrical properties of (PS/SiO_2- $SrTiO_3$) nanocomposites are by calculating both the capacitance and dispersal factor with a device (LCR HiTESTER 3532-50) made from company Hioki at frequencies of (10^2 Hz – 5 MHz) at temperature room, as depicted in the Figure (3.8), in the College of Education for Pure Sciences, Babylon University.

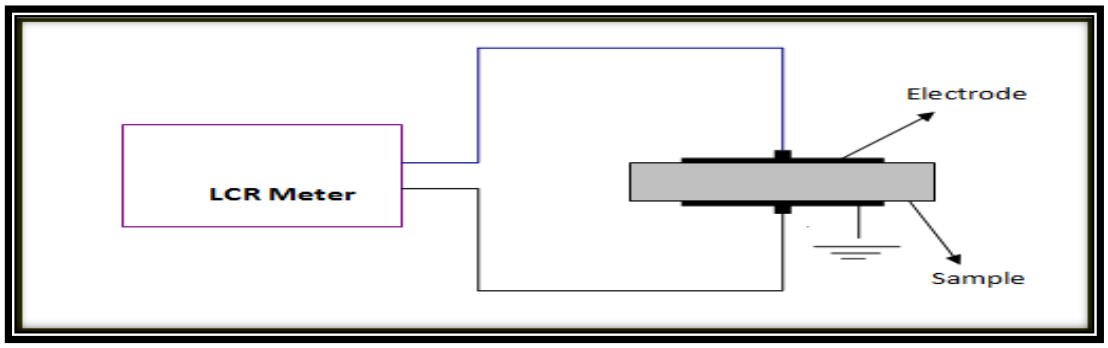

Figure (3.8): Schematic diagram for A.C electrical properties measurement.

3.7 Measurements of Anti-bacterial Activity for Nanocomposites

The disc diffusion technique is used to evaluate the samples of (PS/SiO_2-$SrTiO_3$) nanocomposites for their level of antimicrobial and antibacterial activity. The nanocomposites are tested using the agar diffusion method to evaluate their antimicrobial activity against two different types of clinical bacteria, Escherichia coli and Staphylococcus aureus. When placing the disks of the (PS/SiO_2- $SrTiO_3$) nanocomposites on top of the medium, the mixture is incubated at room temperature for 24 hours. After taking a measurement, the diameter of the inhibitory zone is determined. The samples were examined at the Al-Ameen Center for Research and Advanced Biotechnology in the Holy Shrine. Figure (3.9) shows Staphylococcus aureus bacteria and Figure (3.10) shows Escherichia coli bacteria.

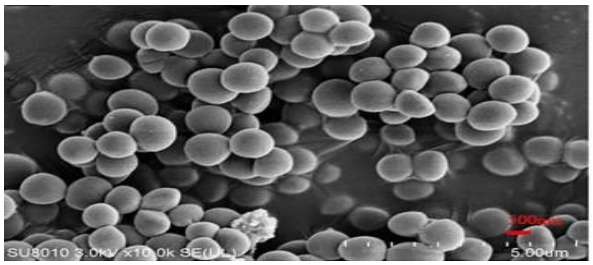

Figure (3.9): Shows Staphylococcus aureus bacteria[88].

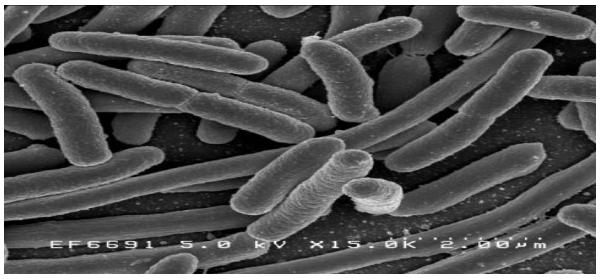

Figure (3.10): Shows Escherichia coli bacteria[89] .

3.8 Measurements of Gamma Ray Shielding for Nanocomposites

Gamma-ray shielding tests of (PS/SiO_2- $SrTiO_3$) nanocomposites are conducted. Test samples are arranged at various concentrations near a gamma ray source (Cs-137, 5μci). The gamma-ray source is located at a distance of 3 cm from the detector, and the samples of nanocomposites are 1cm from the Gamma-ray spring as shown in the Figure (3.11). The Geiger counter uses the samples to calculate the linear attenuation coefficients and transmit gamma-ray fluxes through the samples.

Figure (3.11): Gamma ray shielding.

Chapter Four

Results, Discussion,

And Future works

4.1 Introduction

The chapter included the structural, optical, and alternating current (A.C) electrical measurements and the results and discussion of PS/ SiO_2-$SrTiO_3$ nanocomposites. This chapter also studies the antibacterial activity and gamma-ray radiation applications of PS/ SiO_2-$SrTiO_3$ nanocomposites.

4.2 The Optical Microscope (OM) and Scanning Electronic Microscope (SEM) of (PS/ SiO_2-$SrTiO_3$)

Figure (4.1) shows the optical microscope images of PS/ SiO_2-$SrTiO_3$ nanocomposites taken power a magnification (10X) for samples of different concentrations of SiO_2-$SrTiO_3$ nanoparticles. At low concentration of SiO_2-$SrTiO_3$ NPs, it form of clusters and with increasing concentrations of SiO_2-$SrTiO_3$ nanoparticles a connected network will form inside nanocomposites. The nanoparticles work as charge carriers inside the polymeric structure, changing the material's properties [90]. SEM technology is applied to study the morphology and arrangement of nanocomposites. Figure (4.2) depicts SEM images of PS/ SiO_2-$SrTiO_3$ nanocomposites with varying concentrations of SiO_2-$SrTiO_3$ nanoparticles. With increasing concentrations of SiO_2 and $SrTiO_3$ nanoparticles, the surface morphology becomes more uniform and homogeneous, and the material becomes softer [91]. Nanoparticles in spherical form, similar to grain, are randomly scattered on the surface and near the rough texture. The SEM images depict a network of nanoparticle paths within a polymer matrix [92].

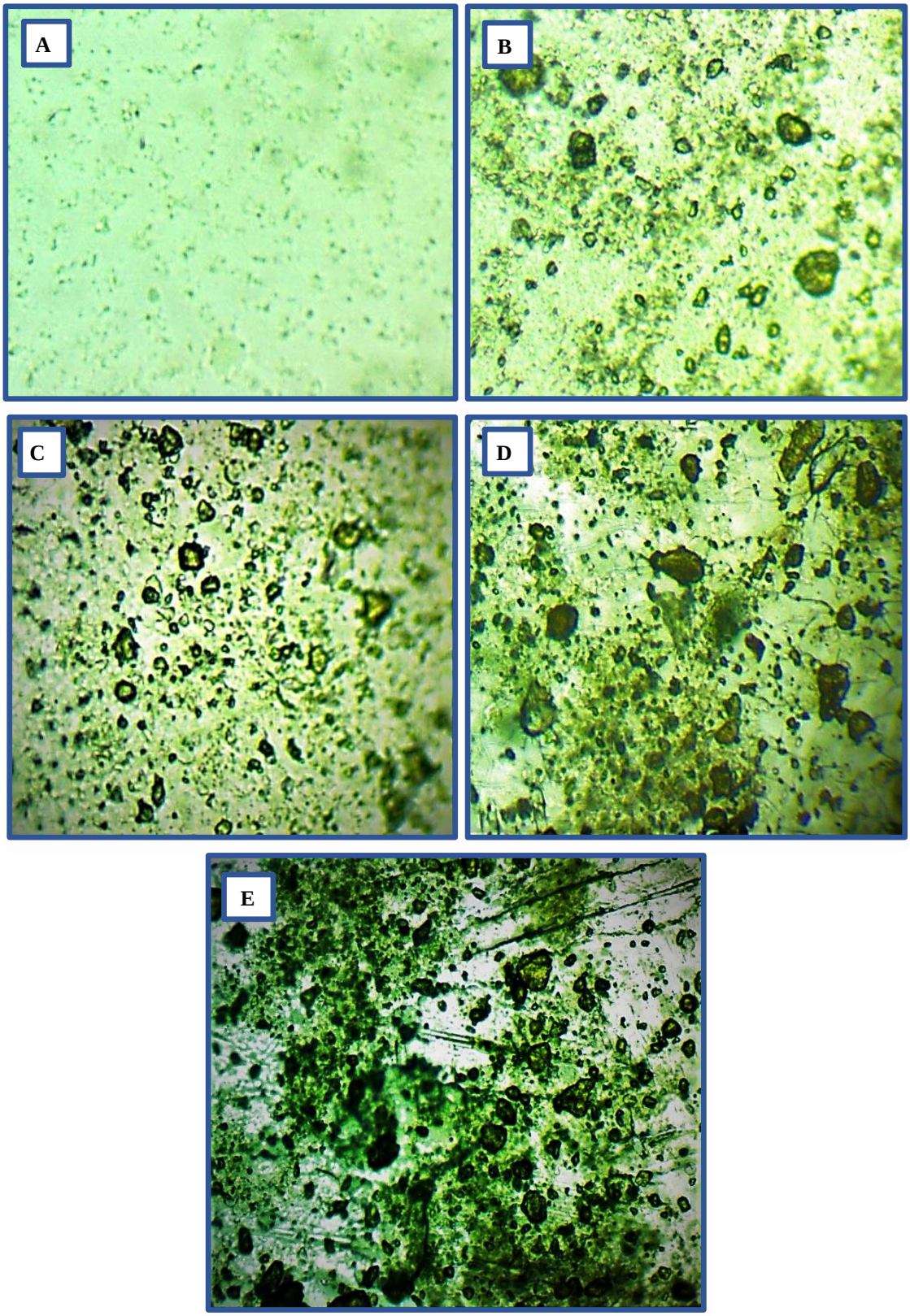

Figure (4.1): The optical microscope images (10X) for (PS/SiO_2-$SrTiO_3$) nanocomposites:(A) for PS, (B) 1.6 wt.% (SiO_2-$SrTiO_3$) NPs, (C) 3.2 wt.% (SiO_2-$SrTiO_3$) NPs, (D) 4.8 wt.% (SiO_2-$SrTiO_3$) NPs, and (E) 6.4 wt.% (SiO_2-$SrTiO_3$) NPs.

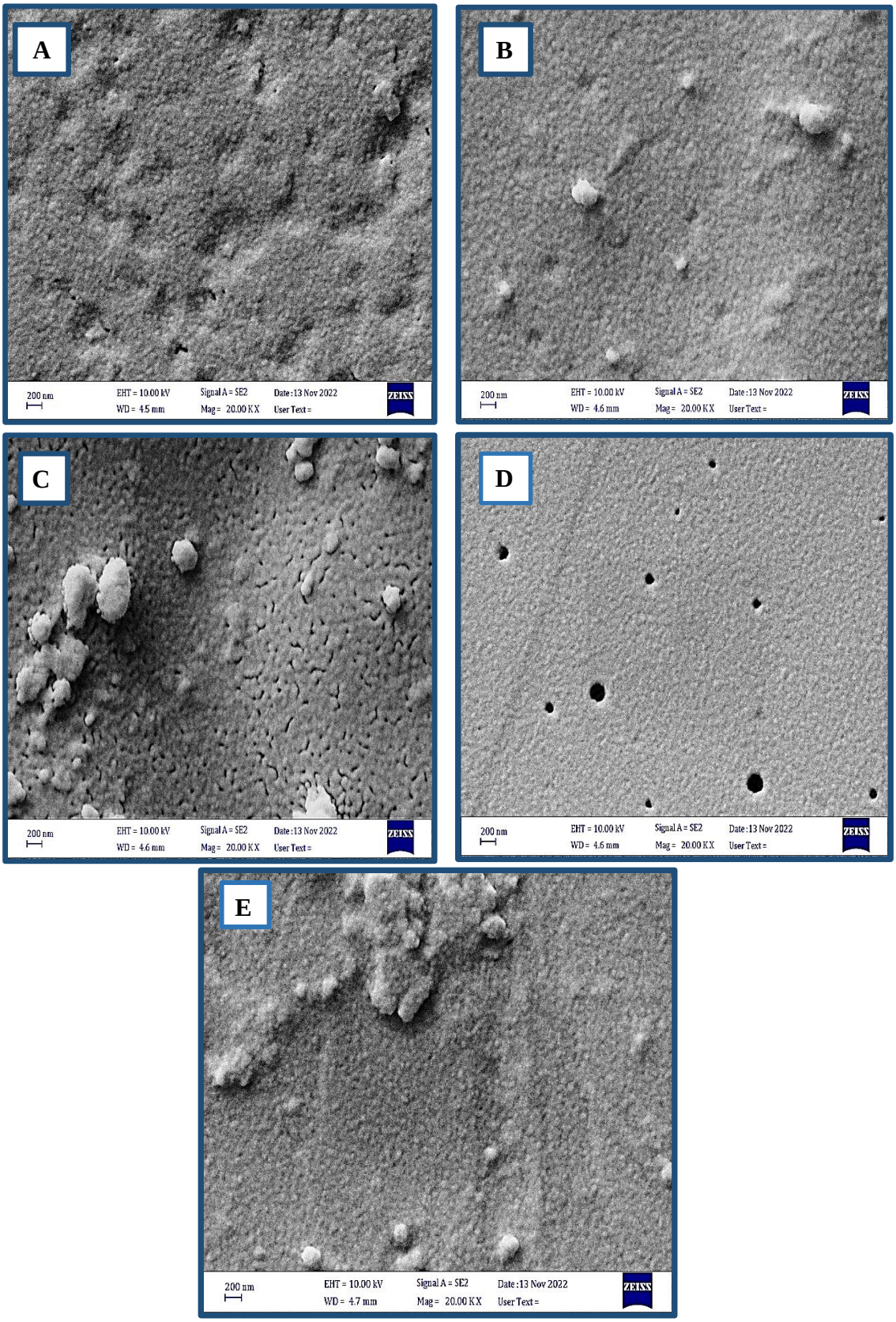

Figure (4.2): The images of (SEM) for (PS/SiO_2-$SrTiO_3$) nanocomposites, A. for PS pure, B. 1.6 wt.% (SiO_2-$SrTiO_3$) NPs, (C) 3.2 wt.% (SiO_2-$SrTiO_3$) NPs, (D) 4.8 wt.% (SiO_2-$SrTiO_3$) NPs and (E) 6.4 wt.% (SiO_2-$SrTiO_3$) NPs.

4.3 Fourier Transform Infrared Ray (FTIR) for (PS/ SiO_2-$SrTiO_3$)

Figure (4.3) shows the (FTIR) transmittance spectra of PS/ SiO_2-$SrTiO_3$ nanocomposites with various contents of SiO_2-$SrTiO_3$ nanoparticles. FTIR spectra revealed interactions in nanocomposites. The wave number 2921 cm^{-1} is allotted to C-H asymmetric stretching vibrations [93]. The bands observed in 1492 cm^{-1} and 1451 cm^{-1} are related to the C=C stretching of the aromatic [94,95]. The bands from 1111 cm^{-1} to 1114 cm^{-1} corresponds to the C-H stretching due to the aromatic ring [96]. The bending vibrational modes of C- H outside the plate of the benzene ring are responsible for two bands that were detected in the ranges of 695 cm^{-1} and 750 cm^{-1}, respectively [97,98], as shown in the table (4.1) . Figure (4.3) is shown that there is no interaction between the polymer (PS) and the nanoparticle (SiO_2-$SrTiO_3$). The nanoparticle (SiO_2-$SrTiO_3$) does not appear in the range 500-4000 cm^{-1} because it is within the wave number of 500 cm^{1}.

Table (4.1): FTIR Transmittance bands positions and their assignments for pure (PS).

Wavenumber (cm^{-1})	Band assignment
2921	C-H asymmetric stretching
1492	C=C stretching
1451	C=C stretching
1111 - 1114	C-H stretching
750	C-H ring
695	C-H ring

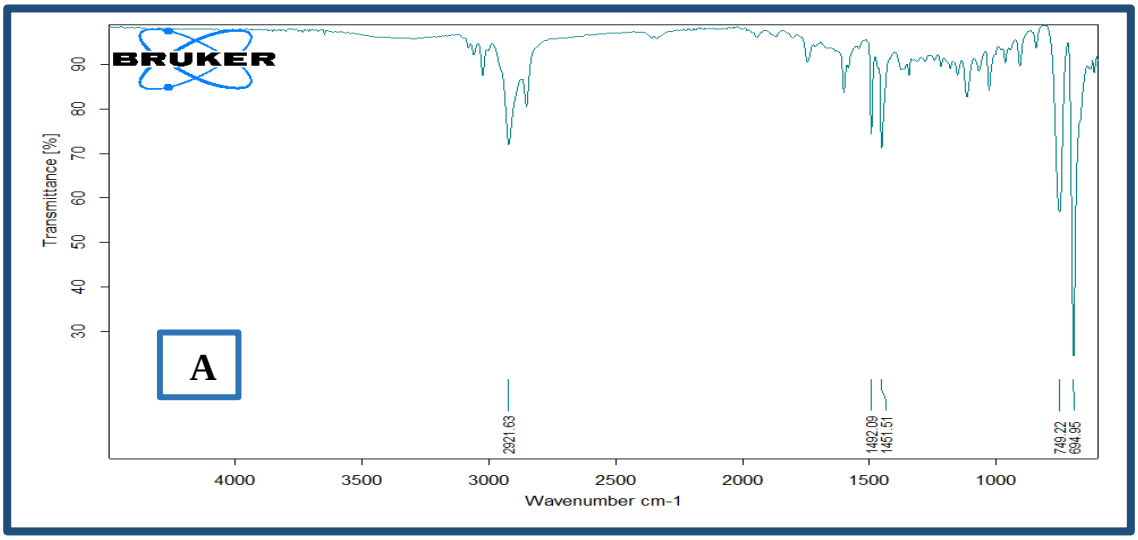
BRUKER
Transmittance [%]
90
80
70
60
50
40
30
A
2921.63
1492.09
1451.51
749.22
694.95
4000
3500
3000
2500
2000
1500
1000
Wavenumber cm-1

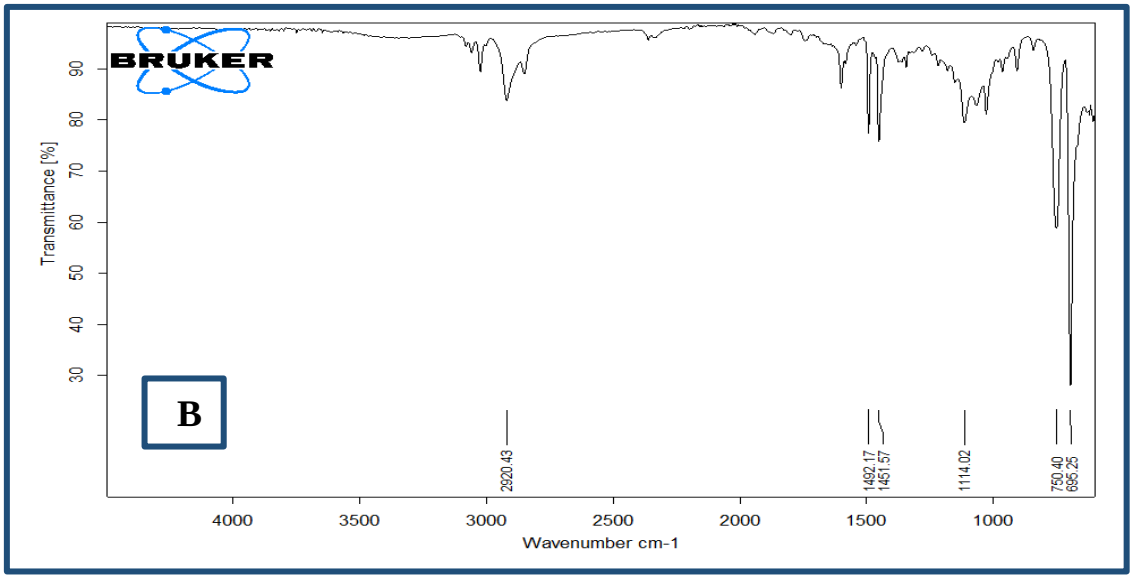
BRUKER
Transmittance [%]
90
80
70
60
50
40
30
B
2920.43
1492.17
1451.57
1114.02
750.40
695.25
4000
3500
3000
2500
2000
1500
1000
Wavenumber cm-1

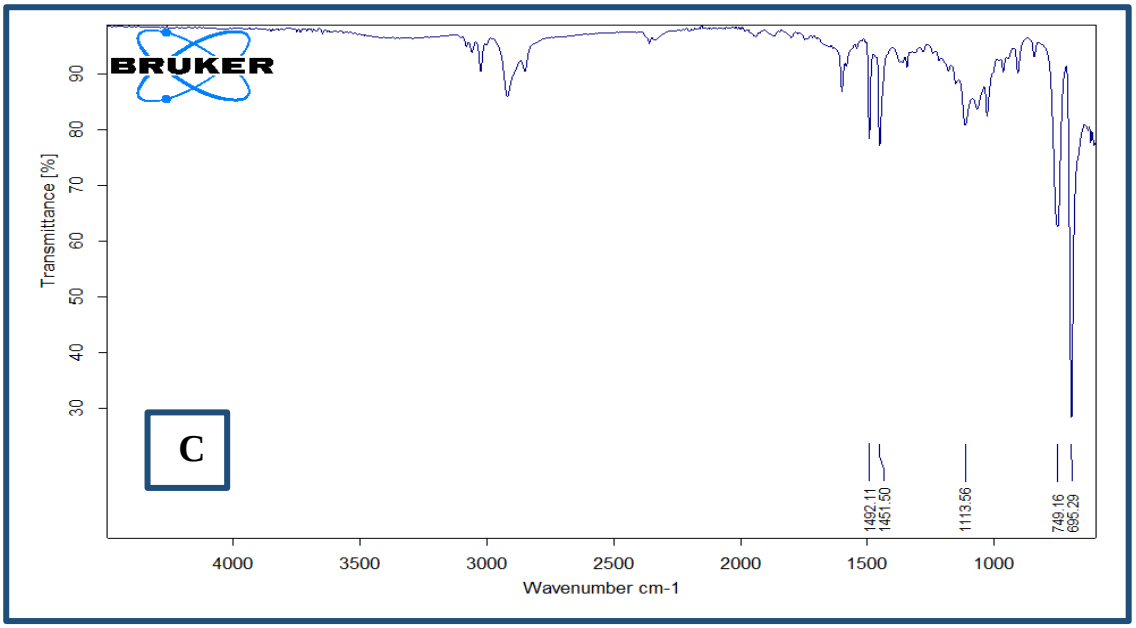
BRUKER
Transmittance [%]
90
80
70
60
50
40
30
C
1492.11
1451.50
1113.56
749.16
695.29
4000
3500
3000
2500
2000
1500
1000
Wavenumber cm-1

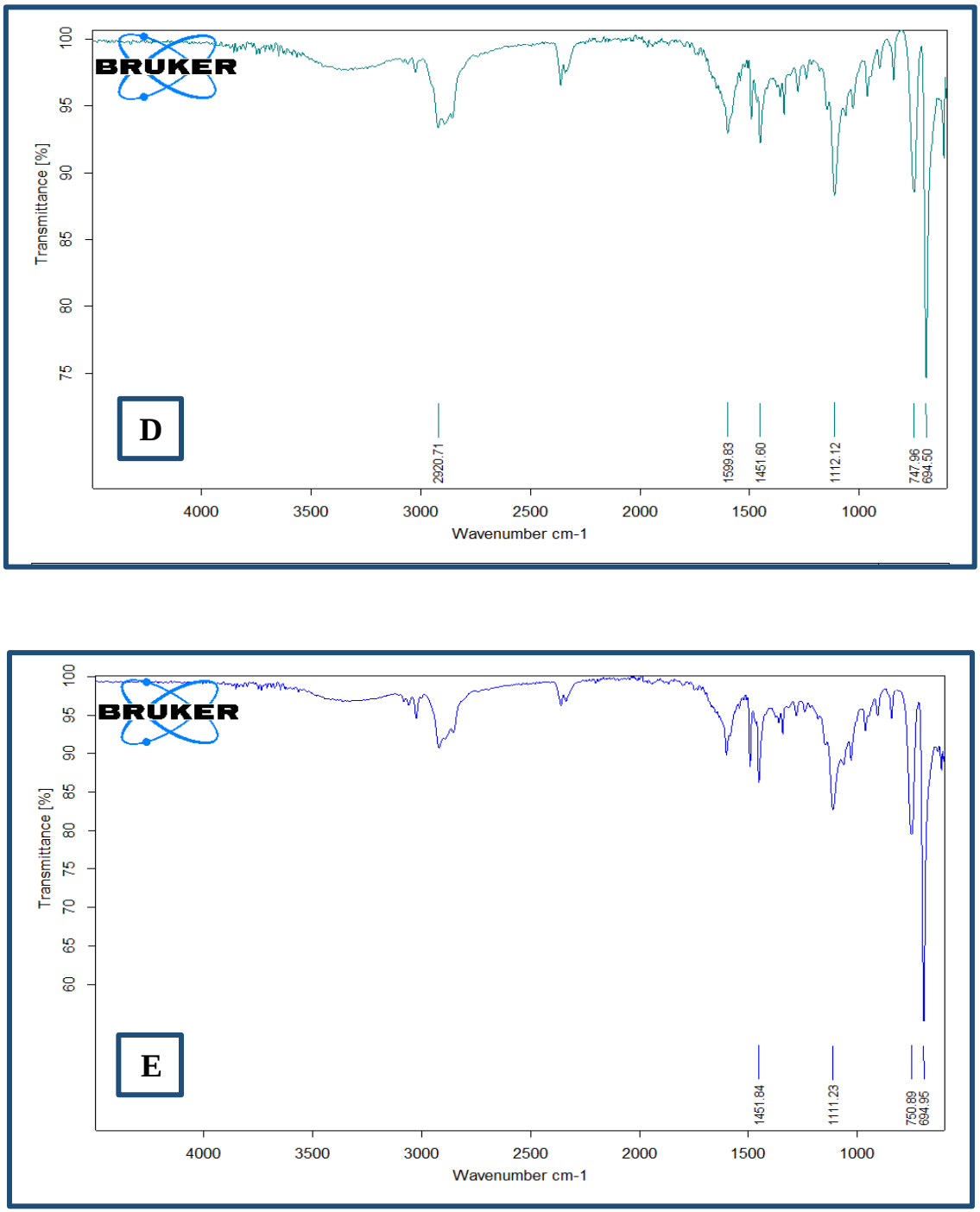

Figure (4.3): FTIR spectra of (PS/SiO_2-$SrTiO_3$) nanocomposites: (A)for PS, (B) 1.6 wt.% (SiO_2-$SrTiO_3$) NPs, (C)3.2 wt.% (SiO_2-$SrTiO_3$) NPs, (D) 4.8 wt.% (SiO_2-$SrTiO_3$) NPs and (E) 6.4 wt.% (SiO_2-$SrTiO_3$) NPs.

4.4 The Optical Properties of (PS/ SiO_2-$SrTiO_3$) Nanocomposites

4.4.1 The Absorbance and Transmittance of (PS/ SiO_2-$SrTiO_3$) Nanocomposites

Figure (4.4) shows the variation of absorbance for PS/SiO_2-$SrTiO_3$ nanocomposites with wavelength, the absorption for the samples of (PS/ SiO_2-$SrTiO_3$) nanocomposites at (UV region) with increasing concentrations for (SiO_2-$SrTiO_3$) nanoparticles. The absorbance for all samples has high values at a wavelength near the fundamental absorption edge (260 nm). Therefore, the absorption falls when the wavelength is increased. High-wavelength incoming photons don't have the energy required to interact with atoms and instead convey electromagnetic radiation. The interaction between the incident photon and the substance will occur when the wavelength lowers, leading to an increase in absorbance. In other words, the free electrons take in the incident light and absorb it. Therefore, absorbance is raised by increasing the weight percentages of nanoparticles [99]. This behaviour agrees with the results of the researchers [100].

Figure (4.5) shows transmittance spectrum of PS/ SiO_2-$SrTiO_3$ nanocomposites against wavelength. The transmittance decreases as the concentricity for (SiO_2-$SrTiO_3$) nanoparticles increases. It is caused by the addition of (SiO_2-$SrTiO_3$) nanoparticles that have electrons in their outermost orbits that travel to high energy levels after sucking electromagnetic energy from incident light. The emission of radiation does not accompany this process because the electron is traveled to more elevated levels and has settled vacant positions in the bands of energy. The light incident in this part is absorbed by the material and does not through it. There are no free electrons since their polystyrene has a high transmittance because

the motion of the electron to the conduction band needs a photon that has high energy [101].

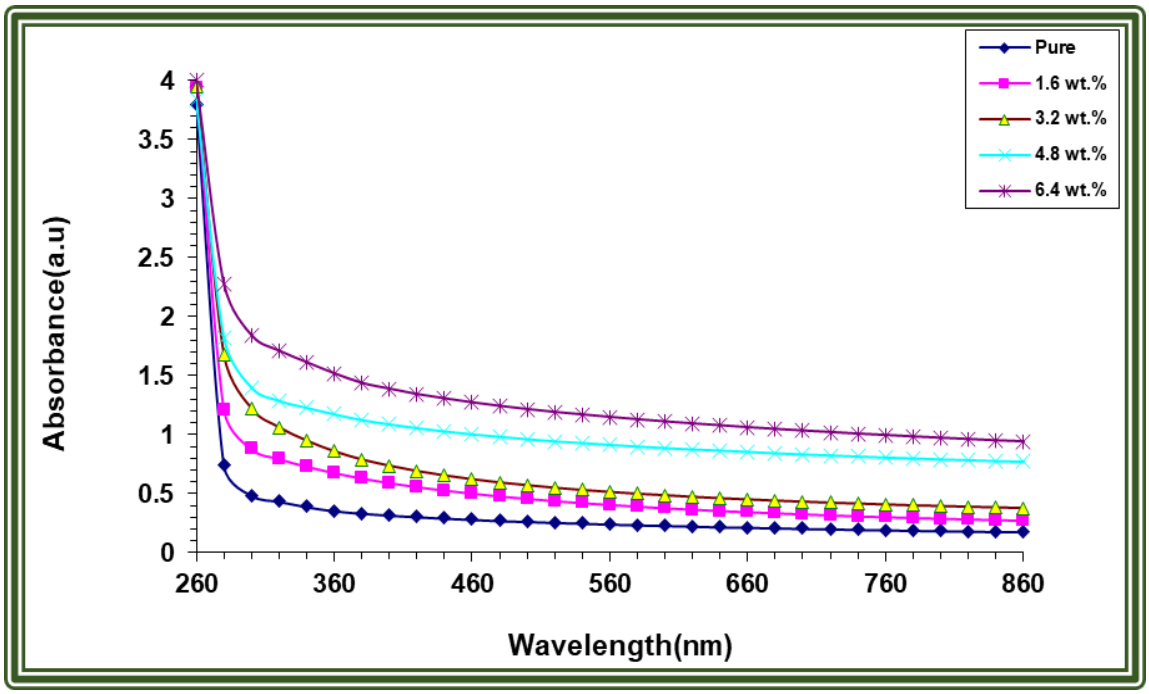

Figure (4.4): Relation between absorbance with wavelength for (PS/SiO_2-$SrTiO_3$) nanocomposites.

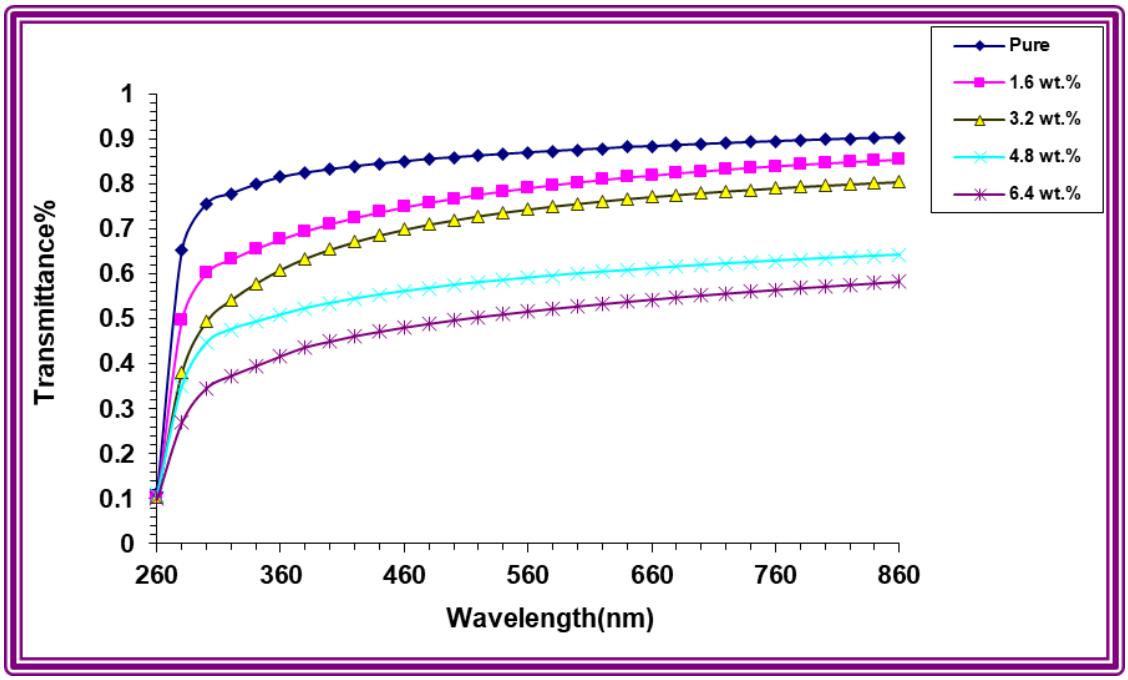

Figure (4.5): Relation between transmittance with wavelength for (PS/SiO_2-$SrTiO_3$) nanocomposites.

4.4.2The Absorption Coefficient for (PS/SiO_2-$SrTiO_3$) Nanocomposites

The absorption coefficient of nanocomposites is calculated by using equation (2.8). Figure (4.6) shows a relation of absorption coefficient (α) with photon energy. The figure shows low α values for the low energies, this indicates a small probability of an electron transition incident photon energy is insufficient to allow an electron to migrate from the valence band (V.B) to the conduction band (C.B) ($h\upsilon < Eg$). The energy of the incident photon is enough to motional the electron from the valence band (V.B) to the conduction band (C.B) at high points, indicating a high probability for electron transitions. This also signifies that the input energy of the photon surpasses the forbidden energy gap. This demonstrates how the absorption coefficient helps define the character of the electron transition. Where is anticipated the electron would transition directly when the absorption coefficient is ($\alpha > 10^4\ cm^{-1}$) at high energies, with conservation of the energy and moment by the photons and electrons. In contrast, in lower energies, where the absorption coefficient is ($\alpha < 10^4\ cm^{-1}$), the electron is anticipated to transition indirectly. The absorption coefficient for PS/SiO_2-$SrTiO_3$ nanocomposites is ($\alpha < 10^4\ cm^{-1}$), which explains why the electron transition is indirect [101].

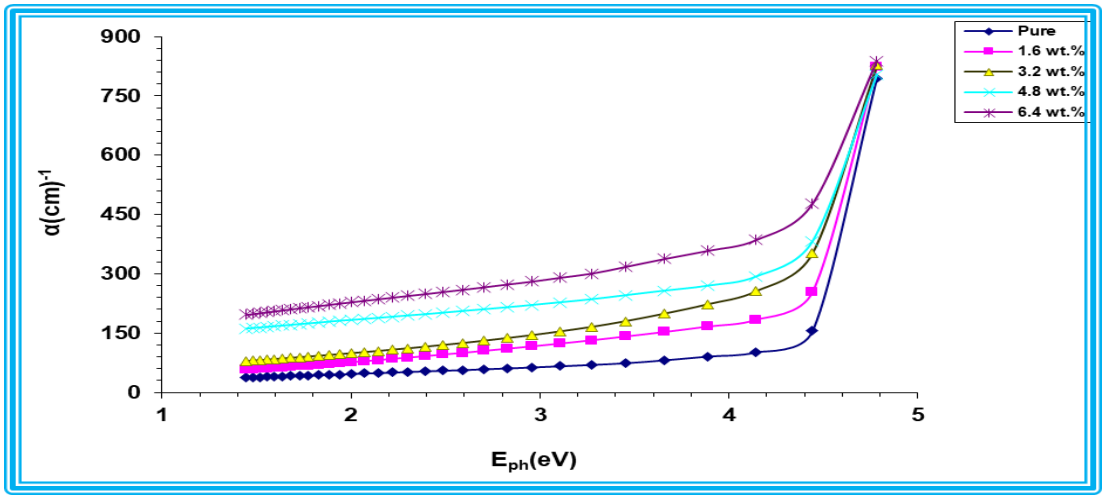

Figure (4.6): Relation between absorption coefficient (α) with photon energy for (PS/SiO_2-$SrTiO_3$) nanocomposites.

4.4.3 Optical energy gap of (PS/SiO_2-$SrTiO_3$)

The energy band gap of nanocomposites is calculated by using equation (2.4). Figures (4.7 and 4.8) show the optical energy gap for the allowed and the forbidden indirect transition, respectively. Where (r = 2) is calculated for the energy gap allowed transition indirectly, and (r = 3)is calculated for the energy gap forbidden transition indirectly. It can observe that when the ratio of SiO_2-$SrTiO_3$ nanoparticles increase, the optical energy gap values decrease, because of the formation of site levels inside the optical energy gap, which caused the electron made a two-transition, the first transition from the valence band (V.B) to the regional levels in the energy gap, and the second transition from the regional levels to the conduction band(C.B) [103]. Table(4.2) provides the energy gap values.

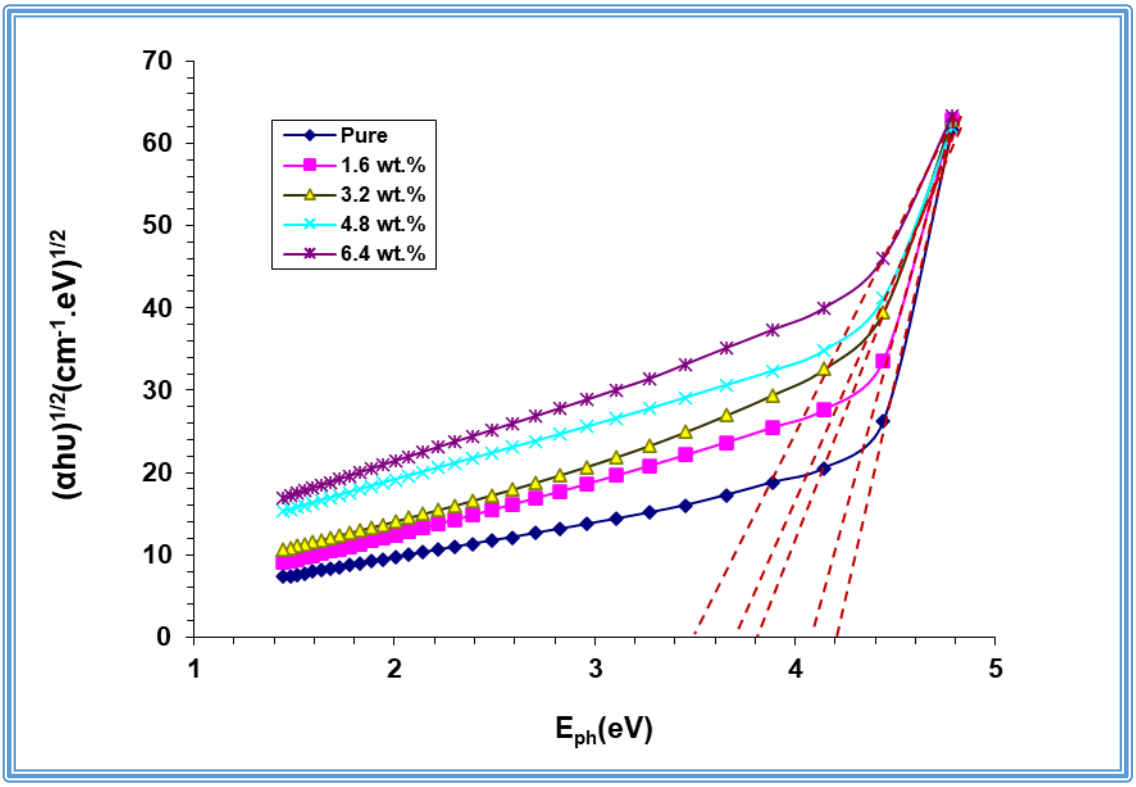

Figure (4.7): Relation between $(\alpha h\upsilon)^{1/2}$ with photon energy for (PS/SiO_2-$SrTiO_3$) nanocomposites.

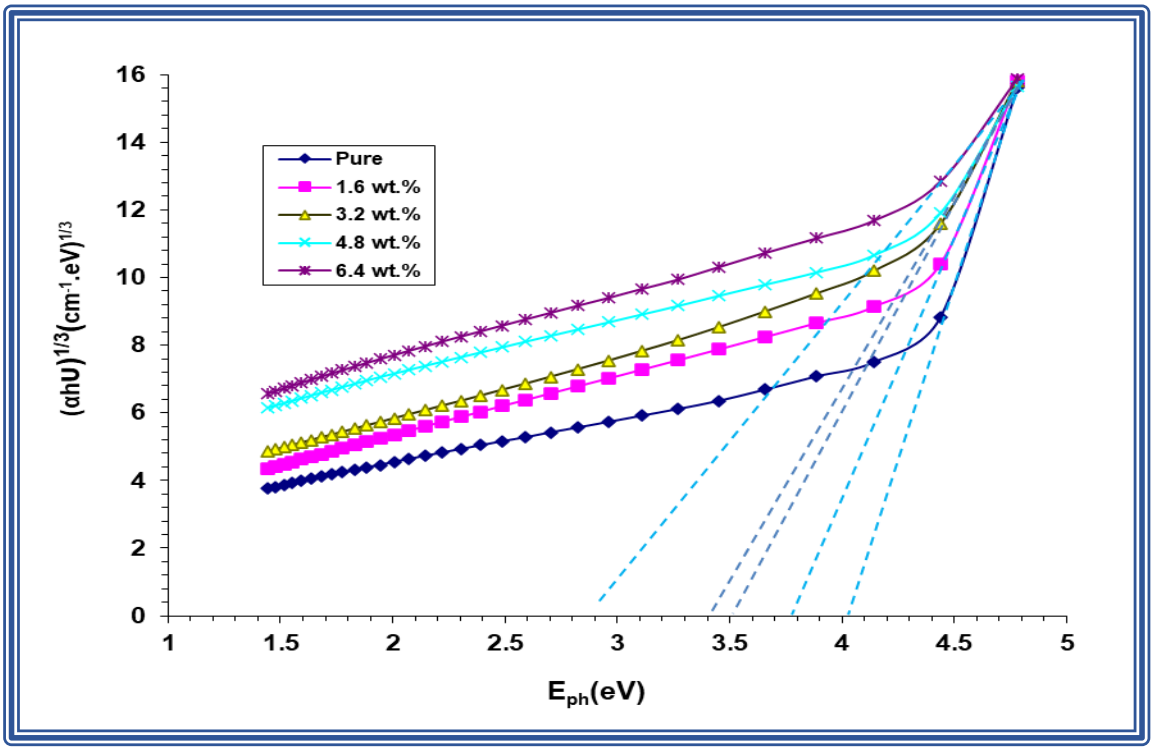

Figure (4.8): Relation between $(\alpha h\upsilon)^{1/3}$ with photon energy for (PS/SiO_2-$SrTiO_3$) nanocomposites.

Table (4.2): The energy gaps values for indirect transitions for allowed and forbidden (PS/SiO_2-$SrTiO_3$) nanocomposites.

(SiO_2-$SrTiO_3$) nanoparticles wt.%	E_g (eV)	
	Allowed	Forbidden
0	4.2	4.03
1.6	4.1	3.77
3.4	3.8	3.5
4.8	3.7	3.4
6.4	3.5	2.9

4.4.4 Extinction Coefficient (k) of (PS/SiO_2-$SrTiO_3$)

The extinction coefficient is calculated by using equation (2.9). The relationship between the extinction coefficient and photon wavelength for (PS/SiO_2-$SrTiO_3$) nanocomposites is shown in figure (4.9). The extinction coefficient shows the ratio of light lost due to a penetration medium's scattering represents absorbance per unit distance and how much absorption loss occurs when electromagnetic waves move through a material. The absorption of a substance and the absorption coefficient are directly correlated with the extinction coefficient [104]. When increasing the concentration of SiO_2-$SrTiO_3$ nanoparticles, the extinction coefficient increasing. This comes from photon dispersion in the matrix of PS and the rise in optical absorption. Due to the high absorbance of all (PS/SiO_2-$SrTiO_3$) nanocomposite samples, the extinction coefficient in the UV region has values higher than the visible region. the extinction coefficient (k) will rise by increasing wavelength because due to the constant of the absorption coefficient of nanocomposites in these areas, almost [105] .

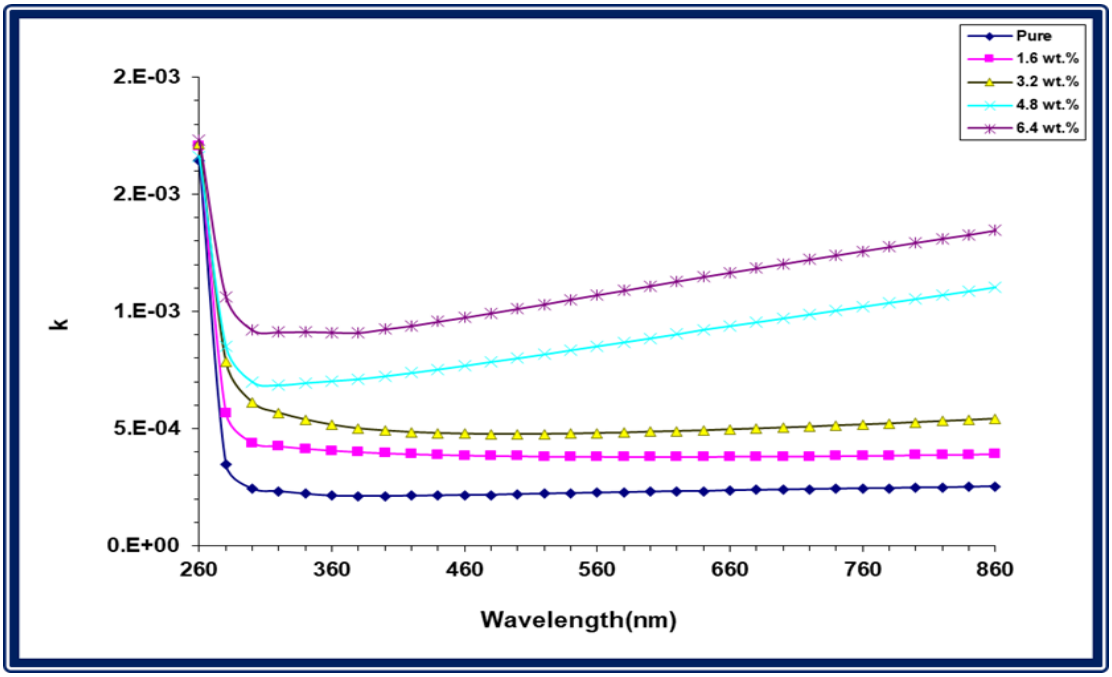

Figure (4.9): Relation between extinction coefficient with wavelength of (PS/SiO_2-$SrTiO_3$) nanocomposites.

4.4.5 Refractive index (n) of (PS/SiO_2-$SrTiO_3$)

The refractive index is calculated by using equation (2.11). Figure (4.10) shows the variation between refractive index with wavelength for (PS/SiO_2-$SrTiO_3$) nanocomposites. Where the increase in concentration (SiO_2-$SrTiO_3$) nanoparticles lead to increase in the refractive index. The refractive index decreases with the increases in the wavelength. This result is explained by the fact that an increase in (SiO_2-$SrTiO_3$) concentration causes an increase in the density of nanocomposites. Due to the poor transmittance in the UV range, high refractive index values are seen there, whereas, in the visible region, low values are seen due to the high transmittance there, this behavior is consistent with the results of the researchers [106,107].

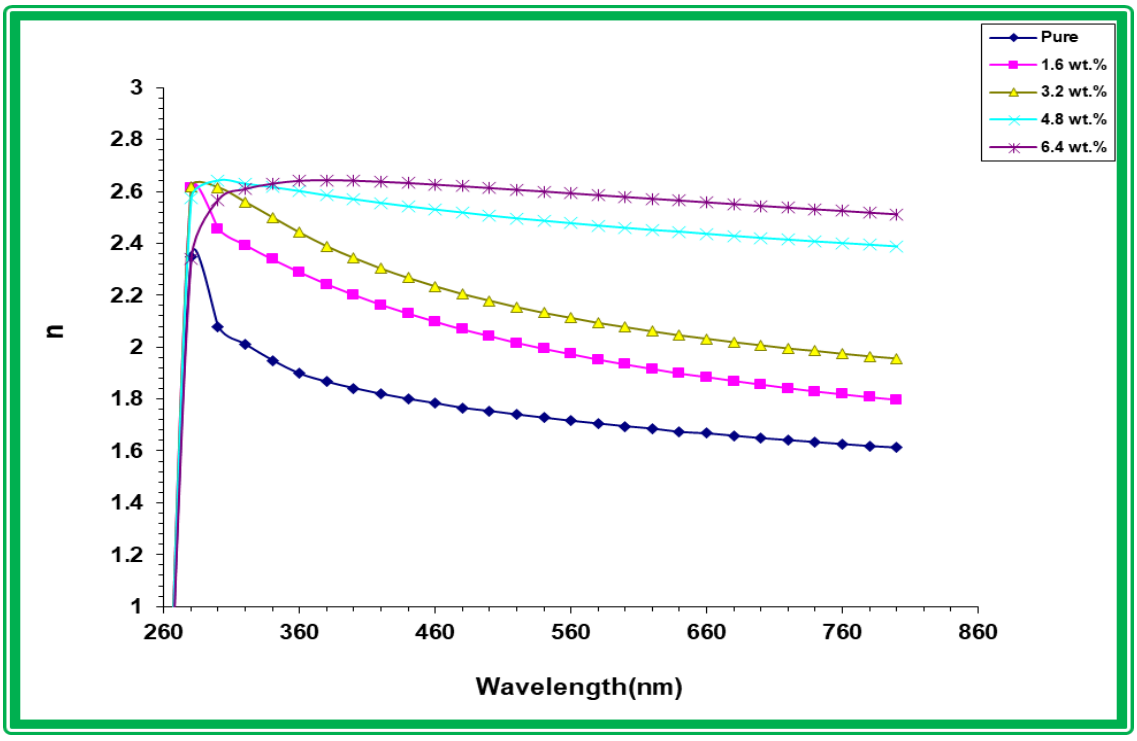

Figure (4.10) : Relation between refractive index with wavelength for (PS/SiO_2-$SrTiO_3$) nanocomposites.

4.4.6 The Real and Imaginary Parts of Dielectric Constant (ε_1, ε_2)

The real and imaginary parts of the dielectric constant are calculated by using equations (2.14) and (2.15), respectively. Figures (4.11) and (4.12) show the relationship between the real part and the imaginary part of the dielectric constant for (PS/SiO_2-$SrTiO_3$) nanocomposites with the wavelength, respectively. From these figures, the real part increases by increasing (SiO_2-$SrTiO_3$) concentration this leads to an increase in refractive index (n) because the real parts of the dielectric constant depend on the refractive index(n), the imaginary parts increase by increasing (SiO_2-$SrTiO_3$) concentration this leads to increase in extinction coefficient (k), and due to depending on the imaginary part of the dielectric constant on the extinction coefficient. Where the extinction coefficient(k) increases with wavelength, particularly in the visible and near infrared wavelength ranges, the effect of the extinction coefficient (k) is relatively small, this conduct is consistent with the results of researchers[108,109] .

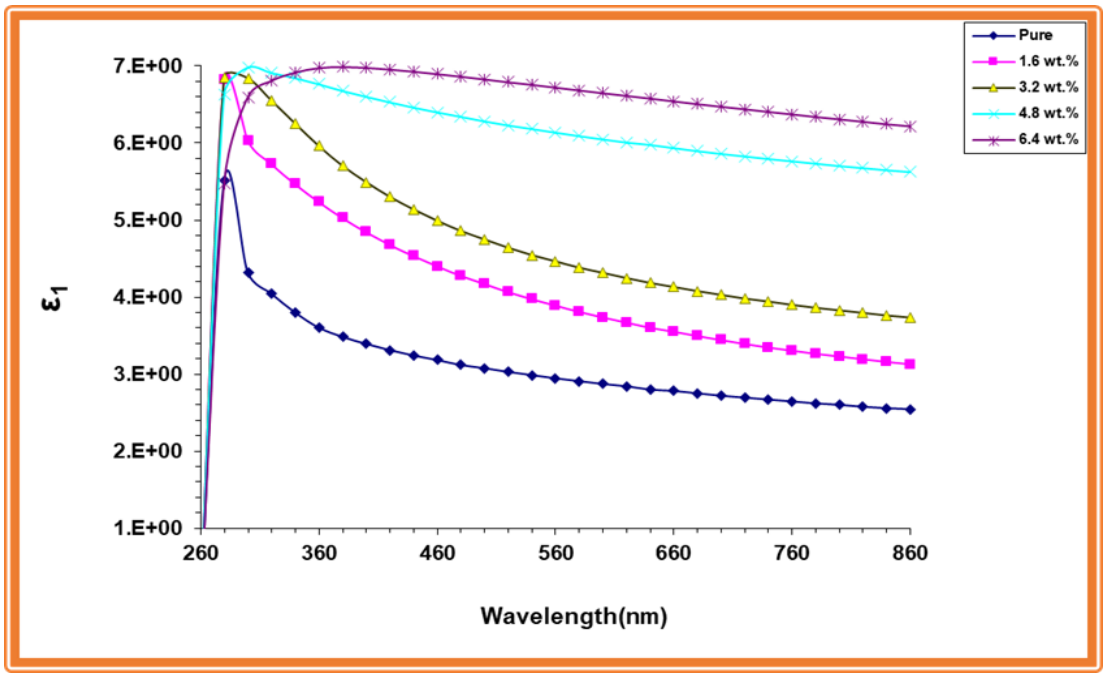

Figure (4.11): Relationship between the part real of the dielectric constant and wavelength for (PS/SiO_2-$SrTiO_3$) nanocomposites.

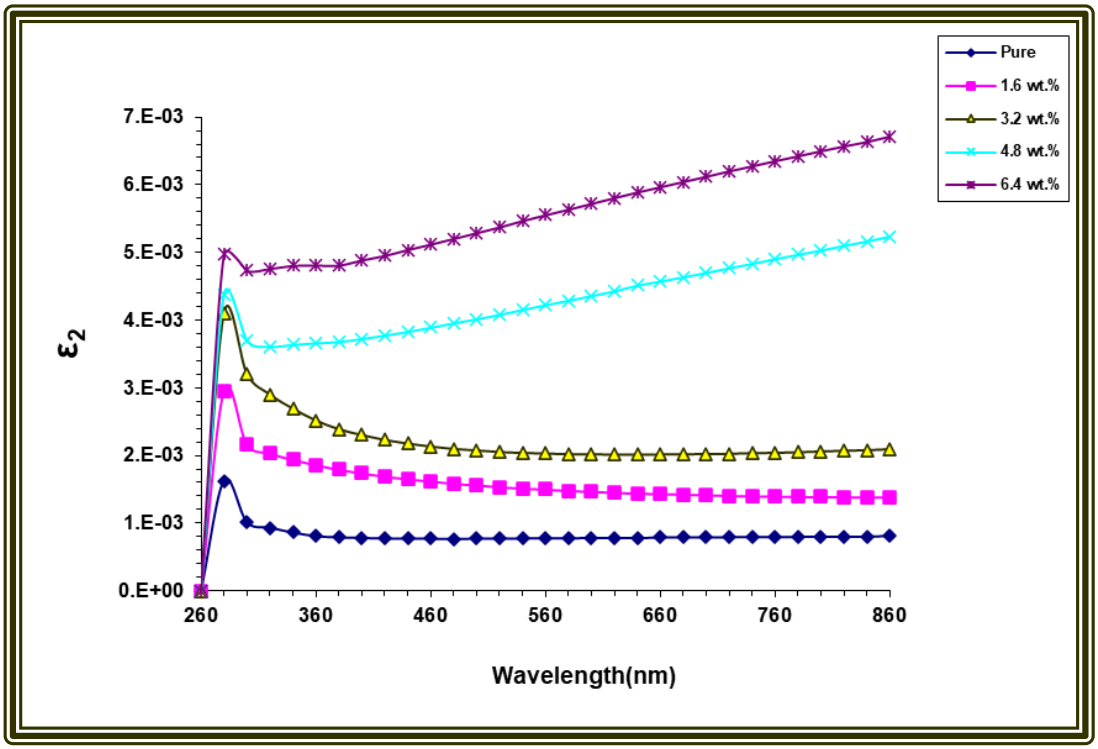

Figure (4.12): Relationship between the part imaginary of the dielectric constant and wavelength for (PS/SiO_2-$SrTiO_3$) nanocomposites.

4.4.7 Optical Conductivity of (PS/SiO_2-$SrTiO_3$)

Figure (4.13) shows the relation ship between optical conductivity and wavelength for (PS/SiO_2-$SrTiO_3$) nanocomposites. Where an increased wavelength of nanocomposites decreased optical conductivity. An increase in optical conductivity is noted by causing an increase in the weight ratio of the concentration of (SiO_2-$SrTiO_3$) NPs to (PS), and these results are consistent with [110 , 111]. This could be caused by an increase in electron transitions between the valence and conduction bands, which contribute more to the decrease of the energy gap and the creation of sit levels[112].

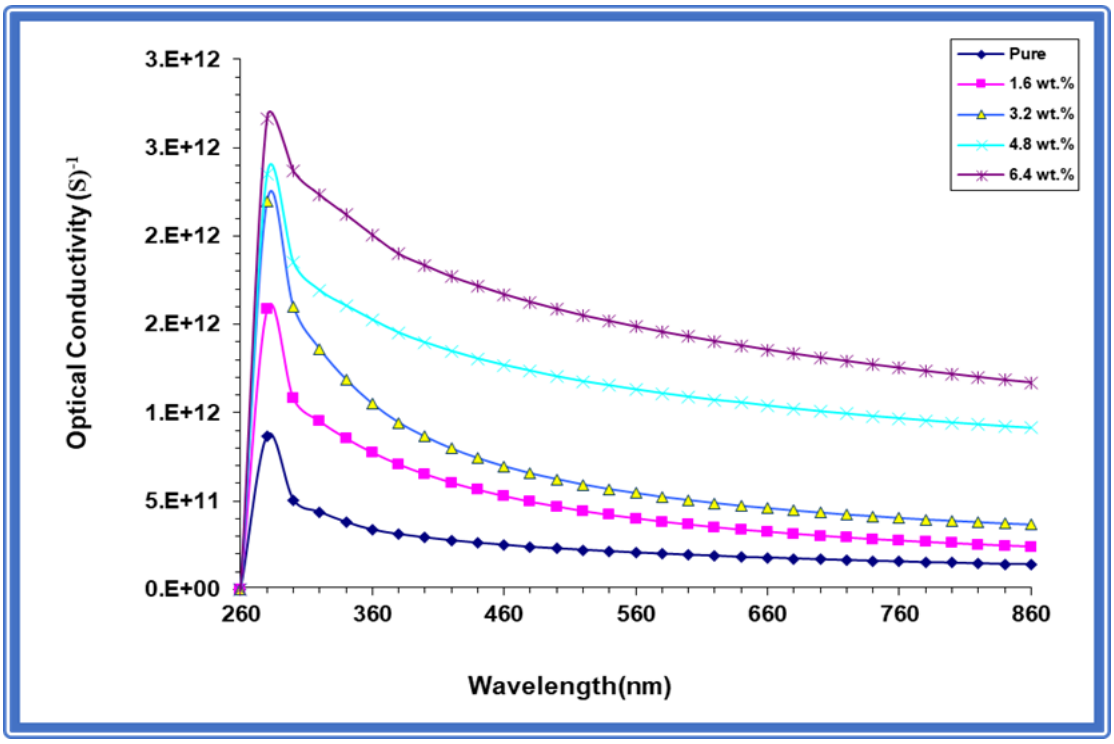

Figure (4.13): Relation between optical conductivity with wavelength for (PS/SiO_2-$SrTiO_3$) nanocomposites.

4.5 The A.C Electrical Properties of (PS/SiO_2-$SrTiO_3$) Nanocomposites

4.5.1 Dielectric constant (ε') and dielectric loss (ε'') of (PS/SiO_2-$SrTiO_3$) nanocomposites

Figures (4.14) and (4.15) demonstrate the relation between the dielectric constant and the dielectric loss with the concentration of (SiO_2-$SrTiO_3$) nanoparticles at room temperature and (100) Hz. The dielectric constant and the dielectric loss of (PS/SiO_2-$SrTiO_3$) are calculated by using equations (2.20) and (2.21), respectively. The (SiO_2-$SrTiO_3$) nanoparticles at low concentrations are determined by darker small regions and become bigger when the (SiO_2-$SrTiO_3$) nanoparticles content increases. At high concentrations of nanoparticles, where will be the network is connected to some and include overlapping paths to allow the charge carriers to pass around. This causes increased dielectric constant and dielectric loss with the concentration of (SiO_2-$SrTiO_3$) NPs due to increasing the free charge carriers and polarized charges ,this result is consistent with [113].

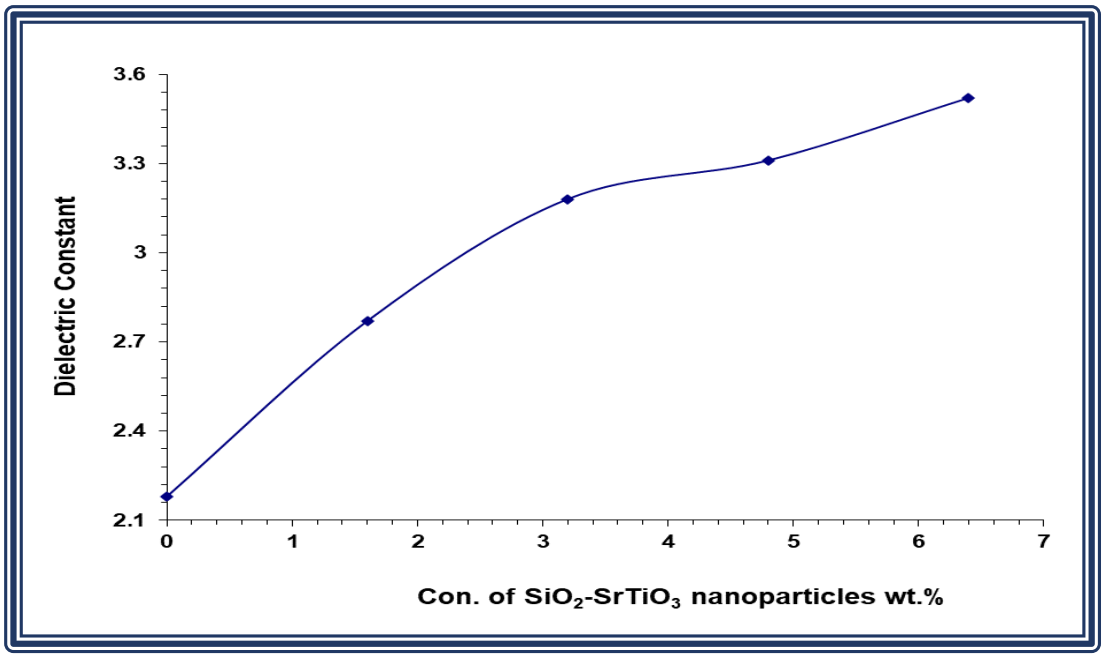

Figure (4.14): Effect of (SiO_2-$SrTiO_3$) nanoparticles concentrations on dielectric constant of PS.

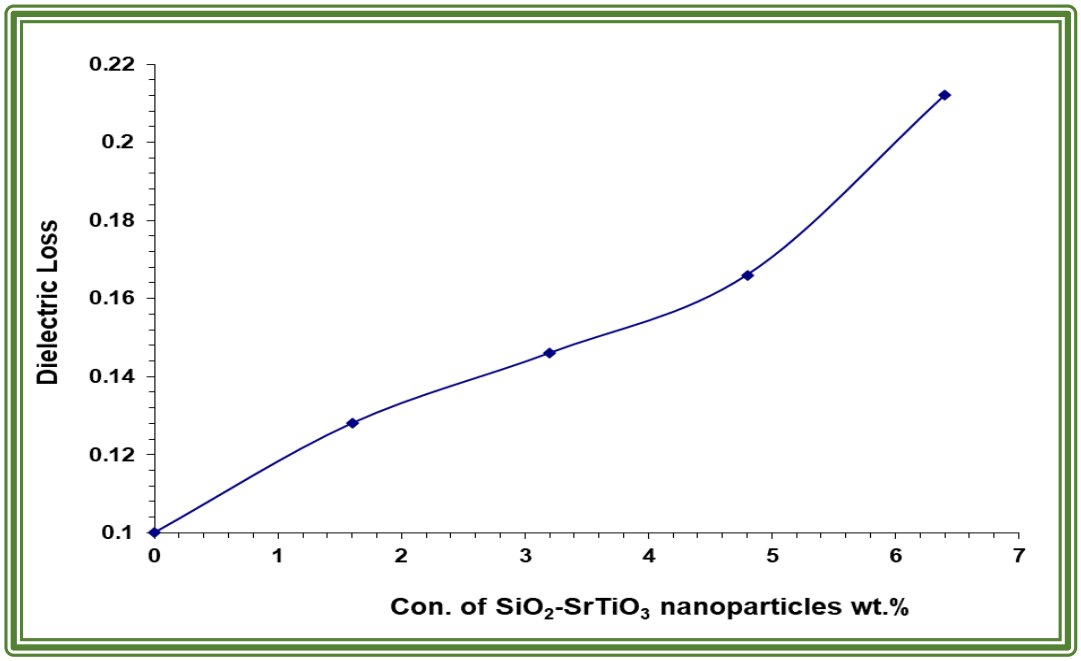

Figure (4.15): Effect of (SiO_2-$SrTiO_3$) nanoparticles concentrations on dielectric of PS.

The dielectric constant and the dielectric loss of the nanocomposite (PS/SiO_2-$SrTiO_3$) decrease as the frequency of the applied field increases, as shown in Figures (4.16) and (4.17). This is because the nanocomposites' dipoles point in the direction of the applied electric field, which results in a reduction of the space charge's polarization relative to the total polarization. At low frequencies, space charge polarization contributes more to polarization, while polarization is lower at higher frequencies. As a result, all samples of (PS/SiO_2-$SrTiO_3$) nanocomposites show a decrease in the dielectric constant and the dielectric loss values as the electric field frequency rises. Also, it can be seen from the figures that for nanocomposites at (f = 4) MHz, ($\mathcal{E}'$) and ($\mathcal{E}''$) grow once again to their greatest values. This high value in dielectric constant and dielectric loss tends to result in the largest absorption. This absorption is brought on by the Maxwell-Wagner phenomenon. This alternating current phenomenon causes enormous dipoles to emerge when charges are forced to align with the field by an externally applied field, this behavior is consistent with the results of researchers [114,115].

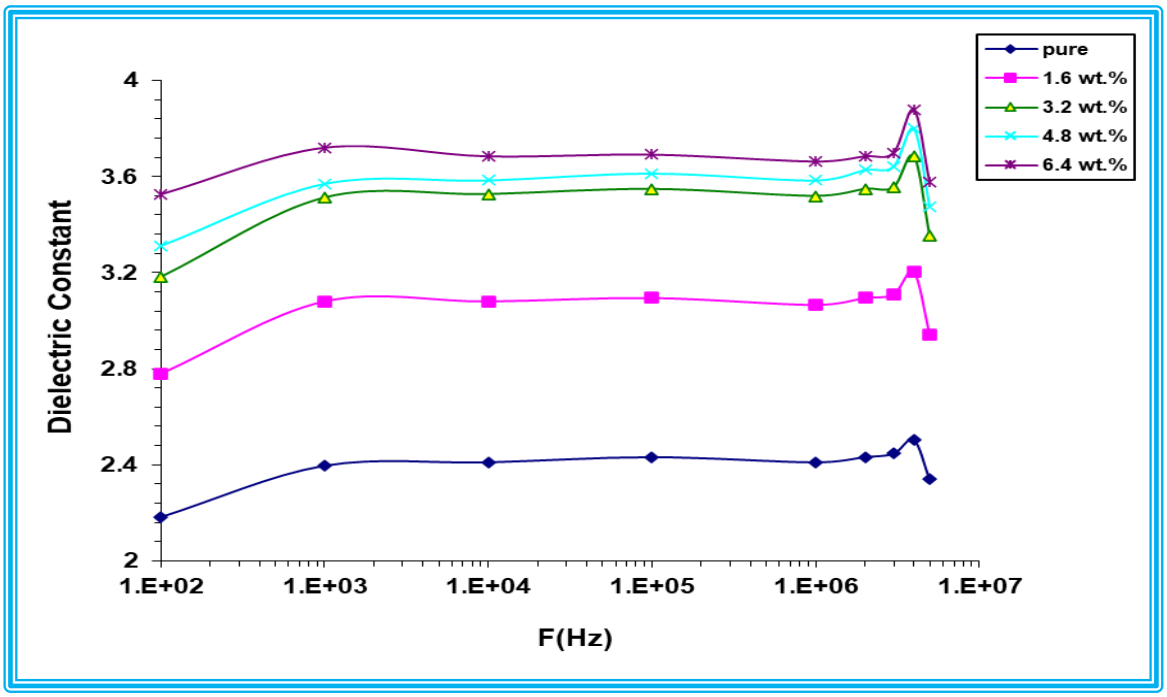

Figure (4.16): Behavior of dielectric constant against frequency for (PS/SiO_2-$SrTiO_3$)nanocomposites.

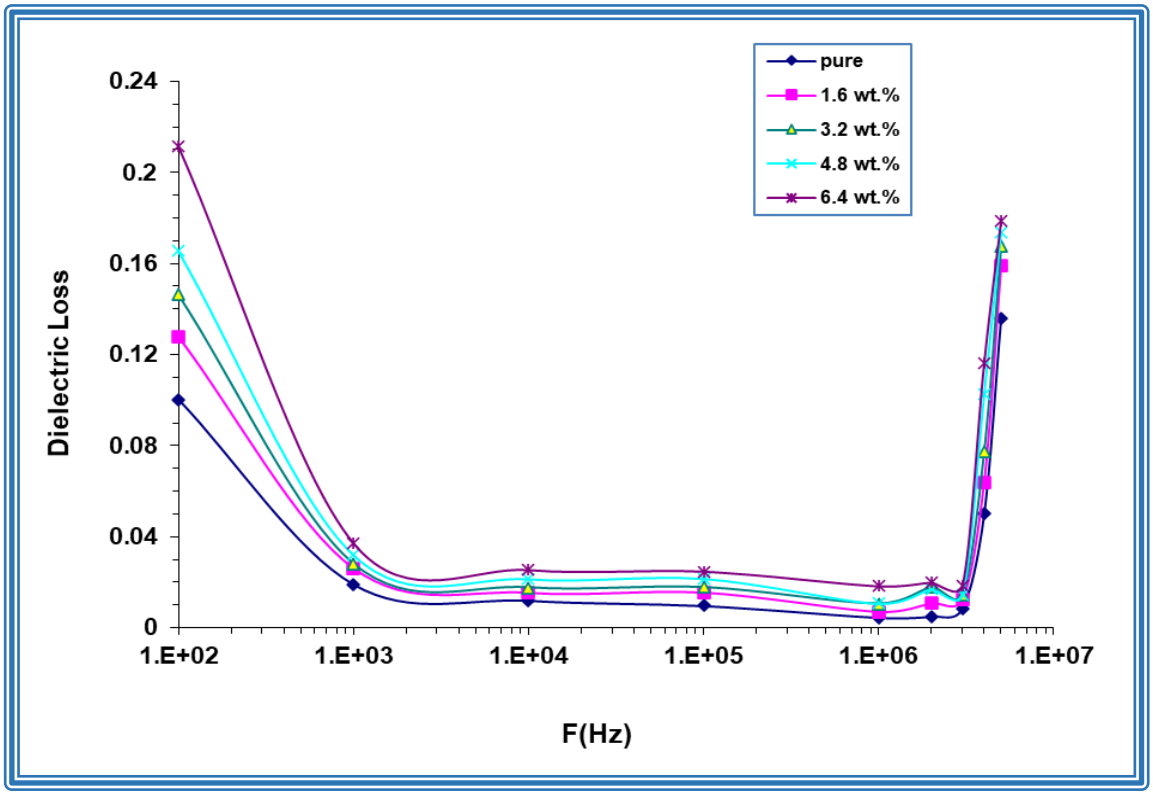

Figure (4.17): Behavior of dielectric loss of (PS/SiO_2-$SrTiO_3$) nanocomposites against frequency.

4.5.2 A.C Electrical conductivity of (PS/SiO_2-$SrTiO_3$) nanocomposites

The A.C conductivity of nanocomposites is calculated by using equation (2.22). Figure (4.18) shows the behavior of A.C conductivity with (SiO_2-$SrTiO_3$) NPs concentration for (PS/SiO_2-$SrTiO_3$) nanocomposites at (100) Hz in room temperature. The conductivity rises with an increase in the (SiO_2-$SrTiO_3$) nanoparticles content. This increase, due to nanoparticles, which increase the number of charge carriers, adds a positional level inside the energy gap, increasing the conductivity[116].

The A.C conductivity for (PS/SiO_2-$SrTiO_3$) nanocomposites varies with frequency, as shown in Figure (4.19). The space charge polarization that takes place at low frequencies and the motion of charge carriers by the hopping process are both responsible for the significant rise in A.C conductivity as frequency increases[117]. As a result, at all contents of (SiO_2-$SrTiO_3$) nanoparticles in (PS/SiO_2-$SrTiO_3$) nanocomposites, conductivity rises as frequency increases.

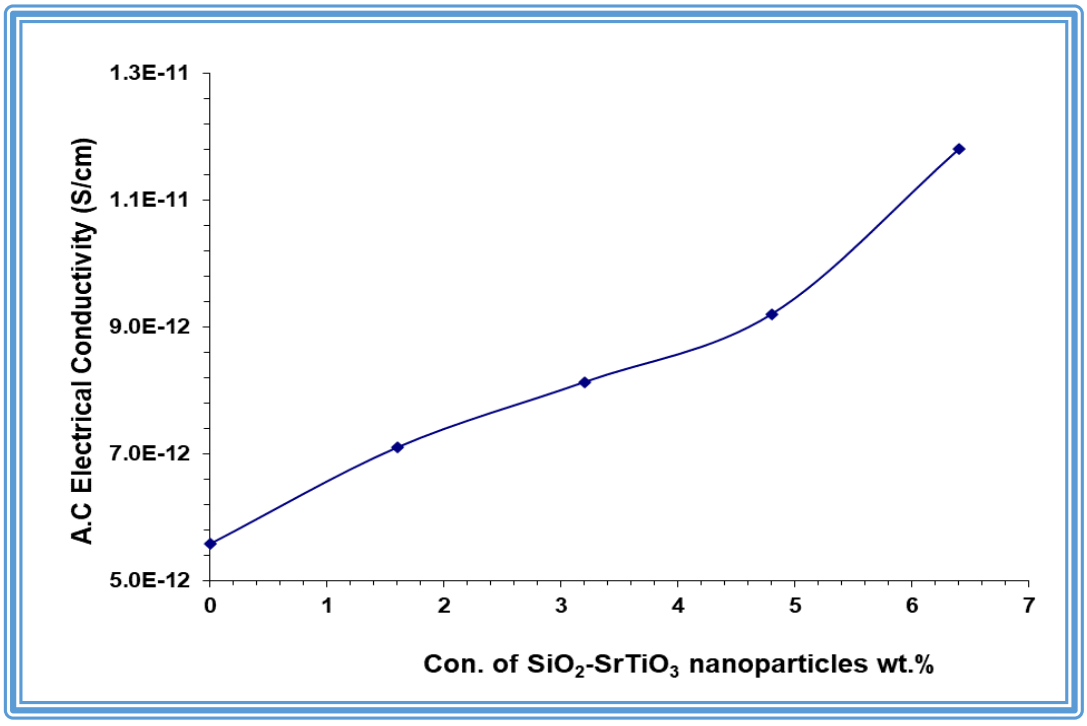

Figure (4.18): Effect of (SiO_2-$SrTiO_3$) nanoparticles concentrations on A.C electrical conductivity of PS.

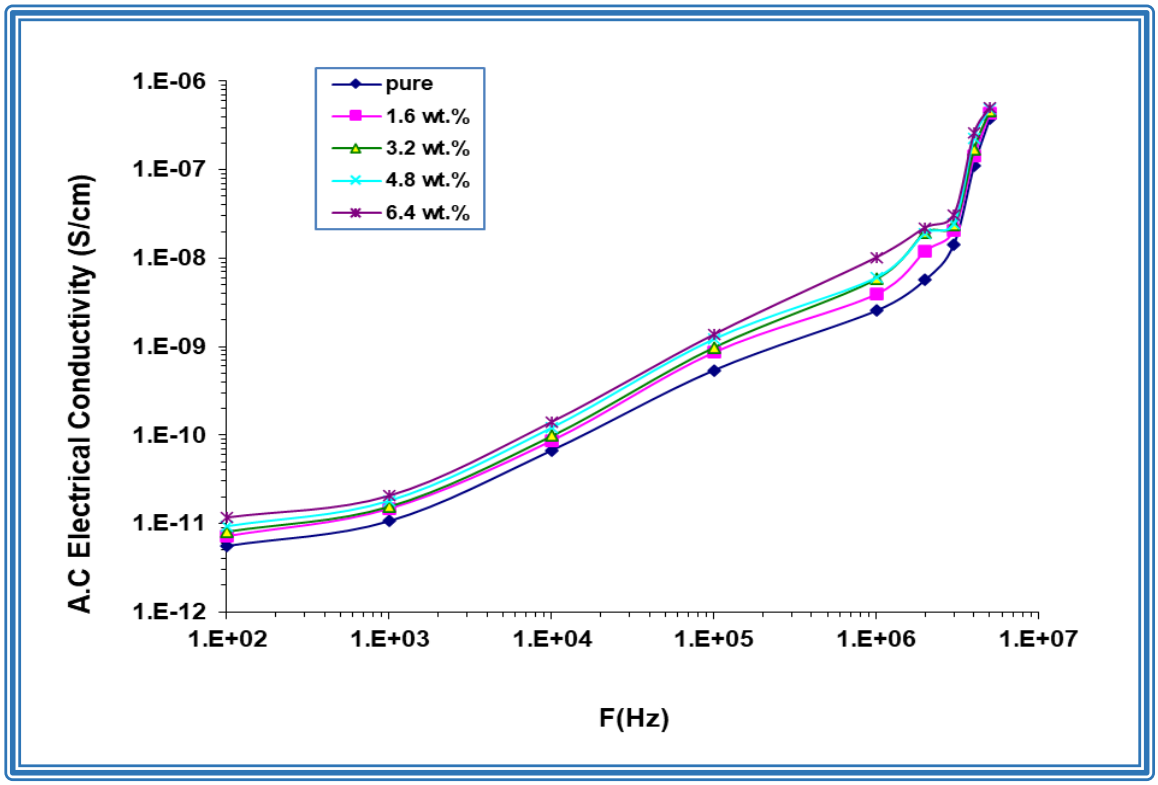

Figure (4.19): Relation between A.C electrical conductivity with frequency for (PS/SiO_2-$SrTiO_3$) nanocomposites.

4.6 Application of (PS/ SiO_2-$SrTiO_3$) Nanocomposites for Antibacterial Activity

Figures (4.20) and (4.21) show tested the agar diffusion technique to assess the inhibition of nanocomposites for antibacterial activity against two types of bacteria, positive-gram (Staphylococcus aureus) and negative-gram (Escherichia coli), respectively. Figure (4.22)and figure (4.23) show the antibacterial properties of the (PS/ SiO_2-$SrTiO_3$) nanocomposites against (S. aureus) and (E. coli) straight. As shown in the figures, by increasing concentrations of SiO_2-$SrTiO_3$ nanoparticles, the inhibition area diameter increases, and these results are consistent with [118].The cause for the antibacterial activity of nanocomposites may be having of reactive oxygen species (ROS) induced by the concentrations of SiO_2 - $SrTiO_3$ nanoparticles that could damage DNA and proteins in bacteria. The possible mechanism

of action is that (PS/ SiO_2-$SrTiO_3$) nanocomposites carry positive charges and bacteria have negative charges that create electromagnetic attraction between microbes and nanoparticles of nanocomposites. When the interaction takes place, the microbes oxidize and die instantly [104]. Table (4.3) shows the inhibition zone diameter of (PS/ SiO_2-$SrTiO_3$) nanocomposites against Staphylococcus and Escherichia coli bacteria.

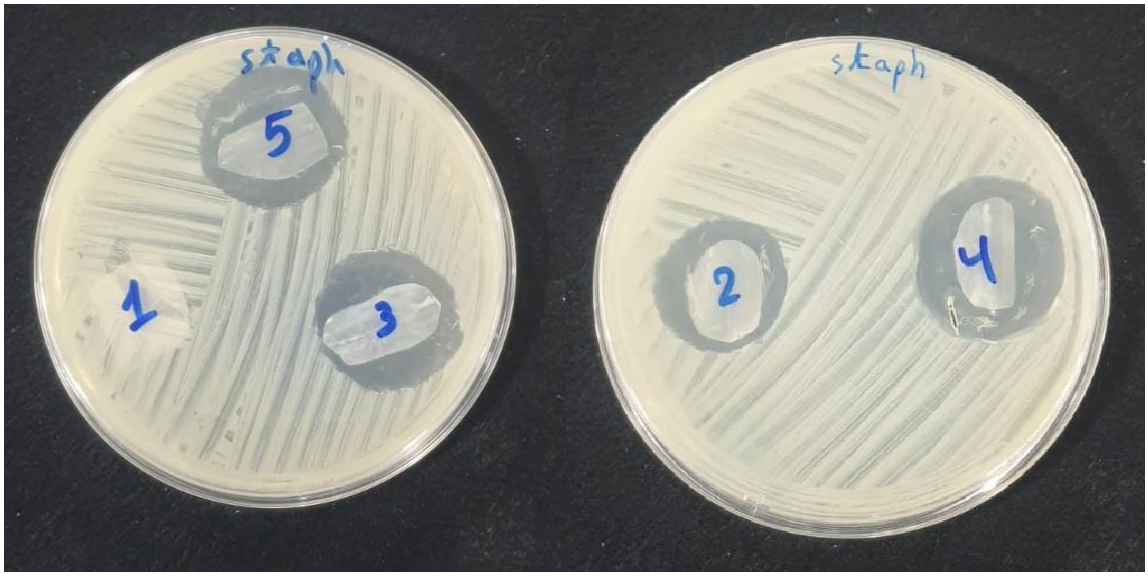

Figure (4.20): Images of inhibition zone for Staph. aureus bacteria.

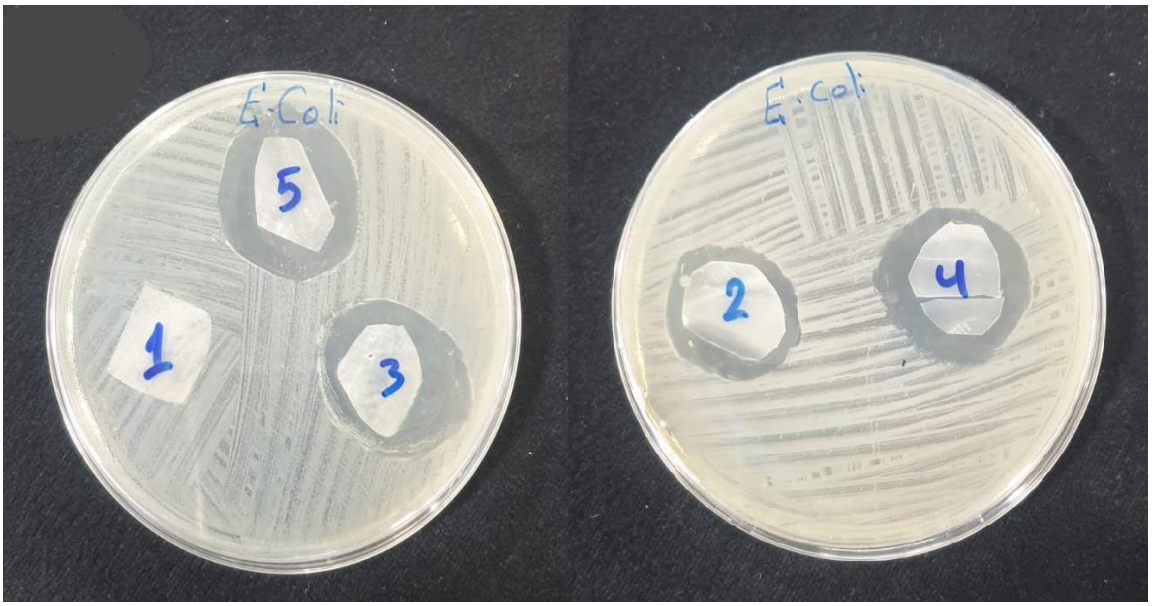

Figure (4.21): Images of inhibition zone for E. coli bacteria.

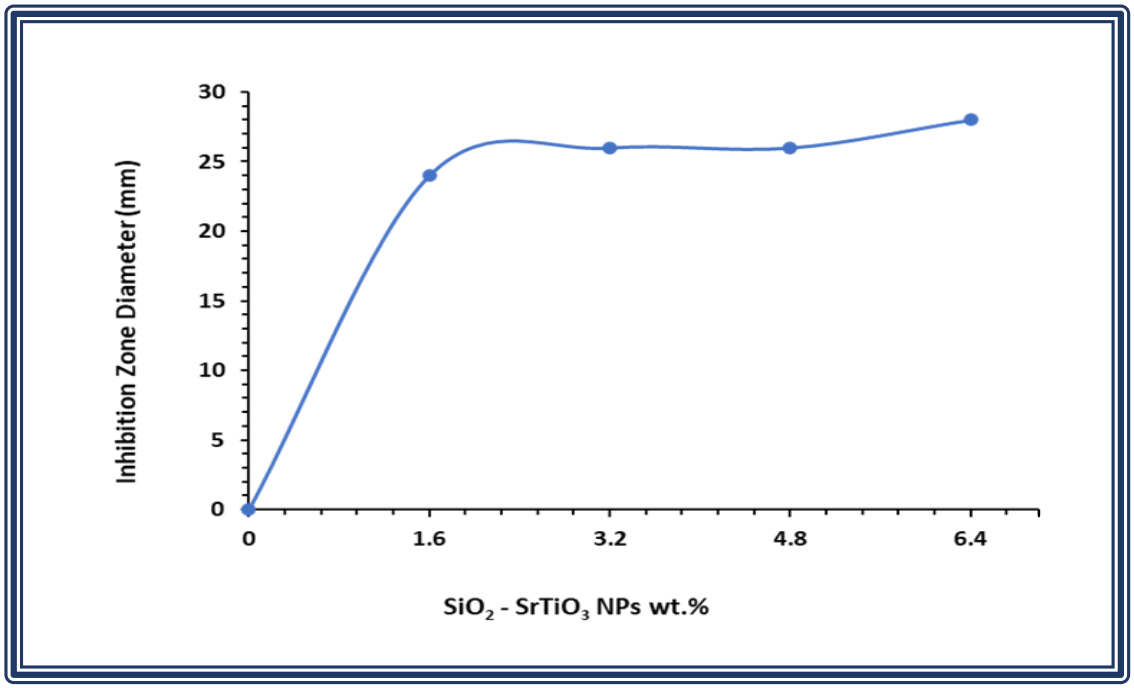

Figure (4.22): Inhibition zone diameter of (PS/ SiO_2-$SrTiO_3$) nanocomposites against (S. aureus) bacterial .

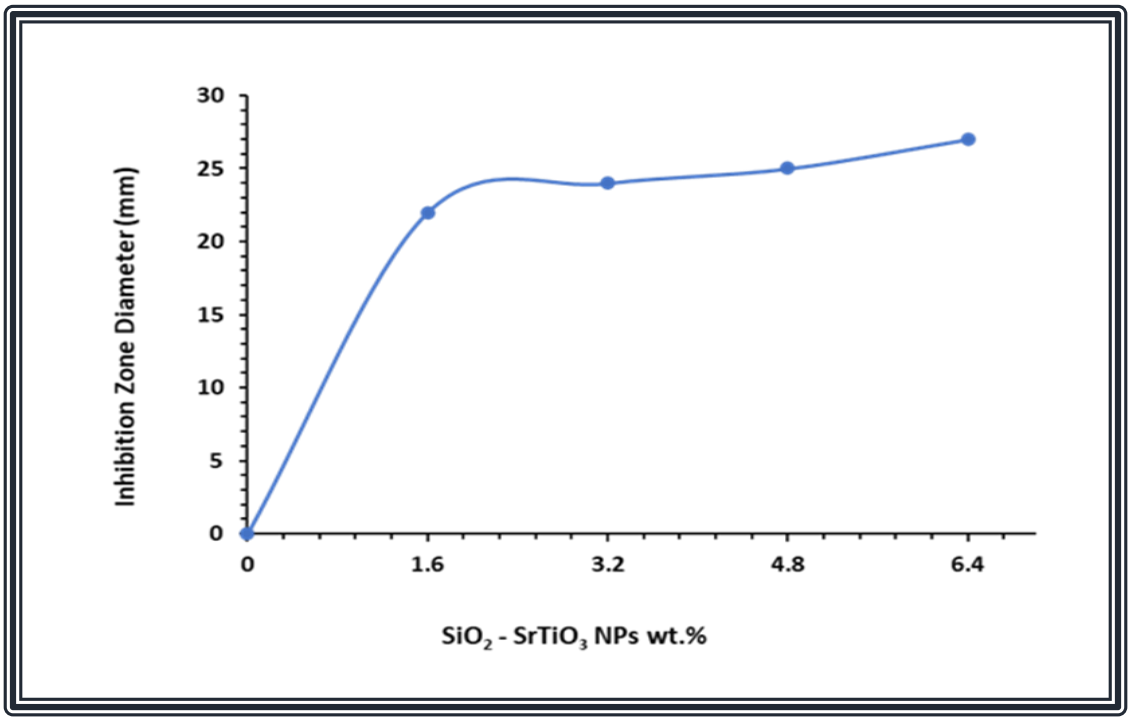

Figure (4.23). Inhibition zone diameter of (PS/ SiO_2-$SrTiO_3$) nanocomposites against (E. coli) bacterial.

Table (4.3): Inhibition zone diameter of (PS/ SiO_2-$SrTiO_3$) nanocomposites.

Number of samples	Nanoparticle concentrations SiO_2-$SrTiO_3$	Staphylococcus aureus(mm)	Escherichia coli(mm)
1	without SiO_2-$SrTiO_3$	0	0
2	with 1.6 wt.%	24	22
3	with 3.4 wt.%	26	24
4	with 4.8 wt.%	26	25
5	with 6.4 wt.%	28	27

4.7 Application of (PS/SiO_2-$SrTiO_3$) nanocomposites for gamma ray shielding

Figure (4.24) depicts the fluctuation in (N/N_o) for concentrations of (PS/SiO_2-$SrTiO_3$) nanocomposites. As shown in this figure, the attenuation radiation increases, due to concentrations increase (SiO_2-$SrTiO_3$) nanoparticles, which is why the transmission radiation drops. The change in gamma attenuation coefficients for the (PS/ SiO_2-$SrTiO_3$) nanocomposites concentrations is shown in Figure (4.25). The attenuation coefficients rise as (SiO_2-$SrTiO_3$) nanoparticles concentrations rise because shielding materials used in nanocomposites either reflect or absorb gamma radiation[119], and is calculated the attenuation coefficients of gamma rays by using equation (2.23).

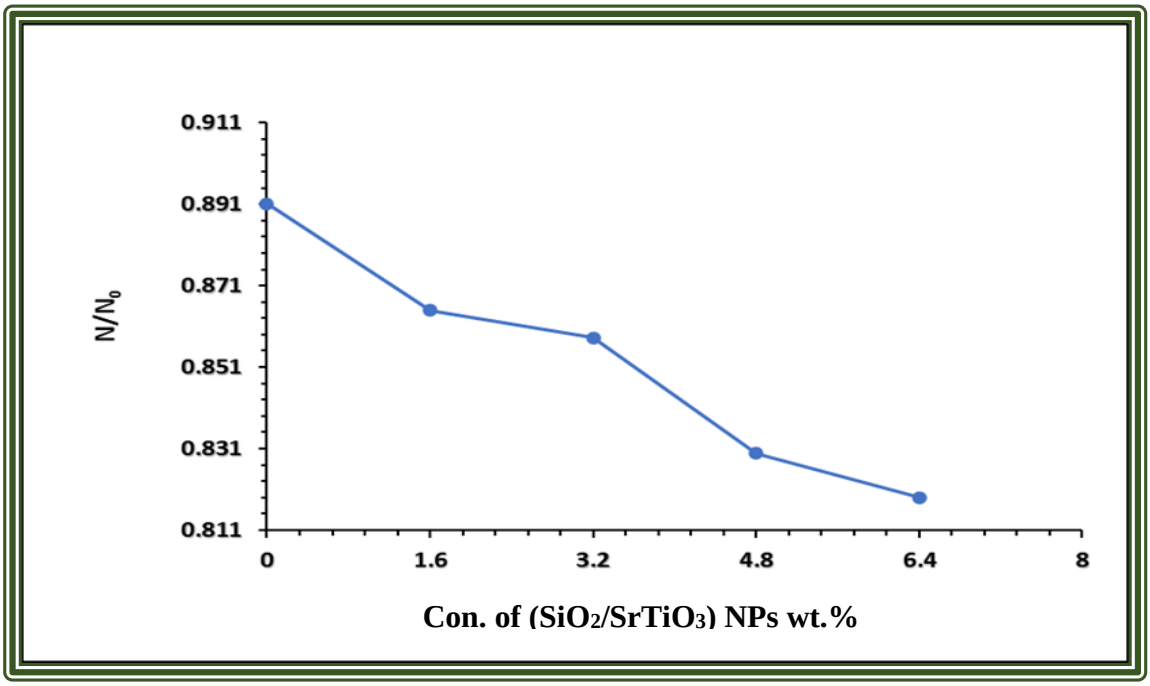

Figure (4.24): Variation of (N/N_0) for (PS/SiO_2-$SrTiO_3$) nanocomposites with different concentrations of (SiO_2-$SrTiO_3$) nanoparticles.

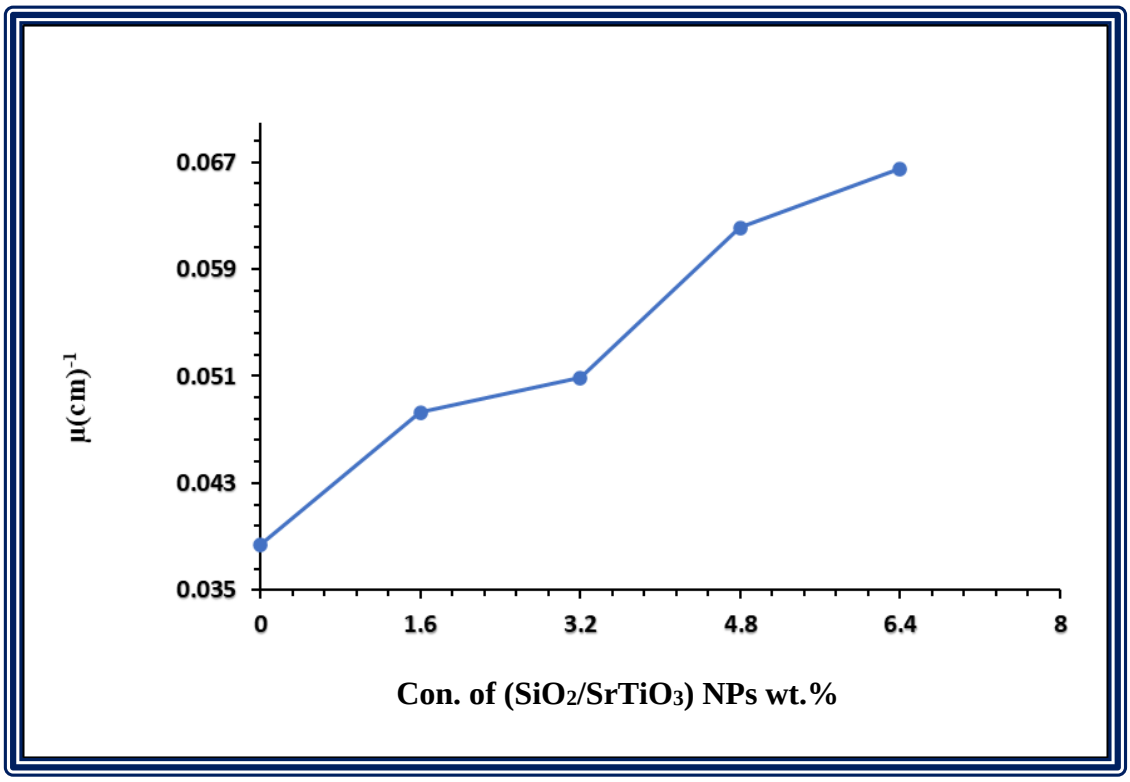

Figure (4.25): Variation of attenuation coefficients of gamma radiation (PS/SiO_2-$SrTiO_3$) nanocomposites with different concentrations of (SiO_2-$SrTiO_3$) nanoparticles.

4.8 Conclusion

1. The optical microscope images showed the homogeneous distribution of nanoparticles (SiO_2 - $SrTiO_3$) in the polymeric matrix. The SEM images showed a homogeneous and good distribution in the surface morphology. through the FTIR measurements that there is a physical superposition between the polymer and the nanoparticles.
2. When increases as (SiO_2 - $SrTiO_3$) nanoparticle concentrations, both increase in absorption, the absorption and extinction coefficients, dielectric constant and real and imaginary parts, optical conductivity, and refractive index of (PS/SiO_2-$SrTiO_3$) nanocomposite, while both energy gap and transmittance decreasing, which can be useful in different optical applications.
3. The dielectric loss for nanocomposites and dielectric constant is decreased with increasing frequency at the same time, which increases the A.C electrical conductivity, if the (SiO_2-$SrTiO_3$) nanoparticles increase, this A.C electrical conductivity, dielectric constant, and dielectric loss of (PS/SiO_2-$SrTiO_3$) nanocomposite increase. This makes it can be used in various electrinos fields.
4. The antibacterial application results for (PS/SiO_2-$SrTiO_3$) nanocomposites show that the inhibition zone for E. coli and S. aureus increases by an increase in concentrations of (SiO_2 - $SrTiO_3$) nanoparticles, suggesting that it may be used for high-activity antibacterial.
5. The linear attenuation coefficients for gamma-ray radiation are increased with an increase in the (SiO_2-$SrTiO_3$) NPs contents.

4.9 Future Work

1. Studying thermal and mechanical properties of nanocomposites (PS/SiO_2-$SrTiO_3$).

2. Studying D.C electrical properties of nanocomposites (PS/SiO_2-$SrTiO_3$).

3. Studying effect of temperature on dielectric properties of (PS/SiO_2-$SrTiO_3$) nanocomposites.

4. Studying of humidity sensors application of (PS/SiO_2-$SrTiO_3$) nanocomposites.

References

References

[1] D. E. Hegazy, M. Eid, and M. Madani, "Effect of Ni nano particles on thermal, optical and electrical behaviour of irradiated PVA/AAc films", Arab J. Nucl. Sci. Appl., vol. 47, no. 1, pp. 41–52, 2014.

[2] A. J. Kadham, D. Hassan, N. Mohammad, and A. Hashim, "Fabrication of (polymer blend-magnesium oxide) nanoparticle and studying their optical properties for optoelectronic applications", Bull. Electr. Eng. Informatics, vol. 7, no. 1, pp. 28–34, doi: 10.11591/eei.v7i1.839,2018.

[3] M. Z. A. Y. A. N. Alias , Z. M. Zabidi A.M.M. Ali, M. K.Harun, "Optical characterization and properties of polymeric materials for optoelectronic and photonic applications", Int. J. Appl. Sci. Technol., vol. 3, no. 5, 2013.

[4] J. R. Fried, "Polymer science & technology": Third Edition. United States of America: Pearson Education, 2014.

[5] A. C. Long, Composites Forming Technologies. New York: CRC Press, 2007.

[6] G. Habi, "Study the effect of gamma ray on the thermal and optical properties of random polymers",M.Sc, Thesis, Babylon University, (2010).

[7] M.Akay, "Introduction to polymer science and technology". Bookboon, 2012.

[8] N. S. Mustafa, M. A. A. Omer, M. E. M. Garlnabi, H. A. Ismail, and C. H. Ch, "Reviewing of general polymer types, properties and application in medical field", Int. J. Sci. Res., vol. 5, no. 8, pp. 212–221, doi: 10.21275/art2016772, 2016.

[9] W. D. Callister, "Materials science and engineering an introduction". New York: John Wiley & Sons, Inc., 2007.

[10] C. W. Tsao and D. L. DeVoe, "Bonding of thermoplastic polymer microfluidics", Microfluid. Nanofluidics, vol. 6, no. 1, pp. 1–16, doi: 10.1007/s10404-008-0361-x, 2009.

References

[11] R. A. Shanks and I. Kong, "General purpose elastomers: structure, chemistry, physics and performance".. doi: 10.1007/978-3-642-20925-3_2, 2013.

[12] C. Li and A. Strachan, "Molecular scale simulations on thermoset polymers: A review", J. Polym. Sci. Part B Polym. Phys., vol. 53, no. 2, pp. 103–122, doi: 10.1002/polb.23489, 2015.

[13] A. Vashchuk, A. M. Fainleib, O. Starostenko, and D. Grande, "Application of ionic liquids in thermosetting polymers: epoxy and cyanate ester resins", Express Polym. Lett., vol. 12, no. 10, pp. 898–917, doi: 10.3144/expresspolymlett.2018.77, 2018.

[14] A. Shrivastava, "Introduction to plastics engineering", in Plastics Design Library, A. B. T.-I. to P. E. Shrivastava, Ed. William Andrew Publishing, pp. 1–16. doi: https://doi.org/10.1016/B978-0-323-39500-7.00001-0, 2018.

[15] R. V. Kulkarni, S. Z. Inamdar, K. K. Das, and M. S. Biradar, "Polysaccharide-based stimuli-sensitive graft copolymers for drug delivery", Elsevier Ltd, doi: 10.1016/B978-0-08-102553-6.00007-6, 2019.

[16] K. Goda, M. S. Sreekala, S. K. Malhotra, K. Joseph, and S. Thomas, "Advances in polymer composites: Biocomposites-state of the art, new challenges, and opportunities", Polym. Compos. Biocomposites, vol. 3, pp. 1–10, doi: 10.1002/9783527674220.ch1, 2013.

[17] A. Hashim, K. H. H. Al-attiyah, and S. F. Obaid, "Modern developments of polymer blend/ oxide nanocomposites for biomedical applications as antibacterial and radiation shielding materials: A Review'', Res. J. Agric. Biol. Sci., vol. 14, no. 1, pp. 8–18, doi: 10.22587/rjabs.2019.14.1.2, 2019.

[18] I. Neitzel, V. Mochalin, and Y. Gogotsi, "Advances in surface chemistry of nanodiamond and nanodiamond-polymer composites",

Second Edi. Elsevier Inc, doi: 10.1016/B978-1-4377-3465-2.00013-X, 2012.

[19] J. Cuppoletti, "Nanocomposites and polymers with analytical Methods. croatia": InTech, 2011.

[20] G. H. Sonawane, S. P. Patil, and S. H. Sonawane, "Nanocomposites and its applications", in Applications of Nanomaterials, Elsevier, pp. 1–22. doi: 10.1016/b978-0-08-101971-9.00001-6, 2018.

[21] M. Joshi and U. Chatterjee, "Polymer nanocomposite: An advanced material for aerospace applications". Elsevier Ltd. doi: 10.1016/b978-0-08-100037-3.00008-0, 2016.

[22] R. O. Ebewele, "Polymer science and technology". New York: CRC Press, 2000.

[23] K. Kik, B. Bukowska, and P. Sicińska, ‘'Polystyrene nanoparticles: Sources, occurrence in the environment, distribution in tissues, accumulation and toxicity to various organisms'’, Environmental Pollution, vol. 262. Elsevier Ltd, Jul. 01. doi: 10.1016/j.envpol.2020.114297, 2020.

[24] B. H. Rabee and I. Oreibi, ''Fabrication of new nanocomposites (PMMA-SPO-PS-TiC) and studying their structural and electrical properties for humidity sensors'’, Bull. Electr. Eng. Informatics, vol. 7, no. 4, pp. 538–546, doi: 10.11591/eei.v7i4.924, 2018.

[25] T. Arfin, M. Faruq, and Nor Azah Yusof, ''Applications of polystyrene and its role as a base in industrial chemistry’', in Polystyrene: Synthesis, Characteristics and Applications, New York: Nova Science Publishers, pp. 269–280, 2014.

[26] J. M. G. Cowie and V. Arrighi, "Polymers: chemistry and physics of modern materials." New York: CRC press, 2007.

[27] B. T. N. C. Andrade, A. C. D. S. Bezerra, and C. R. Calado, ‘'Adding value to polystyrene waste by chemically transforming it into

sulfonated polystyrene'', Rev. Mater., vol. 24, no. 3, doi: 10.1590/s1517-707620190003.0732, 2019.

[28] D.V. Mashtalyar , I.M. Imshinetskiy , K.V. Nadaraia , A.S. Gnedenkov , S.L. Sinebryukhov , A.Yu. Ustinov a , A.V. Samokhin, and , S.V.Gnedenkov, ‘'Influence of ZrO_2/SiO_2 nanomaterial incorporation on the properties of PEO layers on Mg-Mn-Ce alloy'', J. Magnes. Alloy., vol. 10, no. 2, pp. 513–526, doi: 10.1016/j.jma.2021.04.013, 2022.

[29] Vesna V. Vodnik, E. S. Džunuzović, and J. V. Džunuzović, ‘'Synthesis and characterization of polystyrene based nanocomposites’', in Polystyrene: Synthesis, Characteristics and Applications, New York: Nova Science Publishers, pp. 88–100, 2014.

[30] M. Salimi, V. Pirouzfar, and E. Kianfar, '‘Novel nanocomposite membranes prepared with PVC/ABS and silica nanoparticles for C_2H_6/CH_4 separation'', Polym. Sci. - Ser. A, vol. 59, no. 4, pp. 566–574, doi: 10.1134/S0965545X17040071, 2017.

[31] N. F. Muhamad, R. A. Maulat Osman, M. S. Idris, and M. N. Mohd Yasin, ''Physical and electrical properties of $SrTiO_3$ and $SrZrO_3$'', in EPJ Web of Conferences, Nov., vol. 162. doi: 10.1051/epjconf/201716201052, 2017.

[32] M. K. M. Olagunju, X. Poole, P. Blackwelder, M. Thomas, B. Guiton, D. Shukla, J. Cohn, B. Surnar, S. Dhar, E. Zahran, L. Bachas, and, ‘'Size-controlled $SrTiO_3$ nanoparticles photodecorated with Pd cocatalysts for photocatalytic organic dye degradation'', ACS Appl. Nano Mater., vol. 3, no. 5, pp. 4904–4912, doi: 10.1021/acsanm.0c01086, 2020.

[33] U. K. H. Bangi, V. M. Prakshale, W. Han, H. H. Park, N. M. N. Maldar, and L. P. Deshmukh, ‘'Microstructural characteristics of $SrTiO_3$ nanoparticles: The role of capping ligand concentration'', Micro Nano

Lett., vol. 11, no. 5, pp. 273–276, doi: 10.1049/mnl.2015.0531, 2016.

[34] A. C. Marques, ‘'Properties of strontium titanate’'. PhD. Thesis. University of Lisbon, Portugal 11–31, 2009.

[35] N. M. Awad, W. Mekhamer, N. Merghani, A. Hendi, K. Ortashi, and, F.Al-Abbas, ‘'Green synthesis , characterization , and antibacterial activity of silver / polystyrene nanocomposite’', J. ofNanomaterials stirring, vol., pp. 1–6, 2015, doi: 10.1155/2015/943821 ,2015.

[36] M. J. Kadhim, ‘'Effect of nanotitanium on some physical properties of polystyrene films'’,M.Sc. Thesis, Univ. Babylon, 2015.

[37] M. H. Al-Saleh and S. Abdul Jawad, "Graphene nanoplatelet–polystyrene nanocomposite: dielectric and charge storage behaviors'’, J. Electron. Mater., vol. 45, no. 7, pp. 3532–3539, doi: 10.1007/s11664-016-4505-6, 2016.

[38] H. M. Shanshool, M. Yahaya, W. M. M. Yunus, and I. Y. Abdullah, ‘'Investigation of energy band gap in polymer/ZnO nanocomposites'’, J. Mater. Sci. Mater. Electron., vol. 27, no. 9, pp. 9804–9811, doi: 10.1007/s10854-016-5046-8, 2016.

[39] X. Zhang, H. Wen, X. Chen, Y. Wu, and S. Xiao, ‘'Study on the thermal and dielectric properties of $SrTiO_3$/epoxy nanocomposites'’, Energies, vol. 10, no. 5, doi: 10.3390/en10050692, 2017.

[40] S. Moharana, M. K. Mishra, M. Chopkar, and R. N. Mahaling, ‘'Dielectric properties of three-phase PS-$BiFeO_3$-GNP nanocomposites’', Polym. Bull., vol. 74, no. 9, pp. 3707–3719, doi: 10.1007/s00289-017-1914-5, 2017.

[41] D. Hassan and A. Hashim, ''‘Structural and optical properties of (polystyrene–copper oxide) nanocomposites for biological applications’', J. Bionanoscience, vol. 12, pp. 341–345, Jun., doi: 10.1166/jbns.2018.1533,2018.

[42] G. Soni, S. Srivastava, P. Soni, P. Kalotra, and Y. K. Vijay, ''‘Optical,

mechanical and structural properties of PMMA/SiO_2 nanocomposite thin films'', Mater. Res. Express, vol. 5, no. 1, doi: 10.1088/2053-1591/aaa0f7, 2018.

[43] M. A. Habeeb, A. Hashim, and N. Hayder, ‘'Structural and optical properties of novel (PS-Cr_2O_3/ $ZnCoFe_2O_4$) nanocomposites for UV and microwave shielding'', Egypt. J. Chem., vol. 62, no. Part 2, pp. 697–708, doi: 10.21608/ejchem.2019.12439.1774, 2019.

[44] R. Hashim, F. S. Hashim, and E. Al-bermany, ‘'Enhance the optical properties of the synthesis PS- PMMA blend using ZnO/ Fe_2O_3 nanoparticles’, Test Eng. Manag., vol. 83, no. March-April, pp. 21939–21950, 2020.

[45] L. G. L. Weng , L. Liu, X. Wang, X . Zhang , H. Zhang, and, W.Cui, ‘'The effect of Ag@SiO_2 core-shell nanoparticles on the dielectric properties of PVDF based nanocomposites'', Polym. Compos., vol. 41, no. 6, pp. 2245–2253, doi: 10.1002/pc.25535, 2020.

[46] G. Soni, N. Gouttam, and P. Soni, "Optical properties of PMMA/ZnO/SiO_2 composite thin film", Mater. Today Proc., vol. 30, pp. 35–38, 2020.

[47] B. H. Rabee and R. Haider, ‘'The effect of adding Ag nanoparticles on the electrical properties (A.C) of the PMMA-SPO-PS blend'', J. Phys. Conf. Ser., vol. 1973, no. 1, doi: 10.1088/1742-6596/1973/1/012102, 2021.

[48] L. H. Gaabour, ‘'Effect of addition of TiO_2nanoparticles on structural and dielectric properties of polystyrene/polyvinyl chloride polymer blend’', AIP Adv., vol. 11, no. 10, Oct., doi: 10.1063/5.0062445, 2021.

[49] O. B. Fadil and A. Hashim, ''‘Fabrication and tailored optical characteristics of CeO_2/SiO_2 nanostructures doped PMMA for electronics and optics fields’', Silicon, vol. 14, no. 15, pp. 9845–9852, doi: 10.1007/s12633-022-01728-1, 2022.

[50] M. H. Meteab, A. Hashim, and B. H. Rabee, ‘'Controlling the Structural and Dielectric Characteristics of PS-PC/Co_2O_3-SiC Hybrid nanocomposites for nanoelectronics applications’', Silicon, doi: 10.1007/s12633-022-02020-y, 2022.

[51] S. K. Sharma, D. S. Verma, L. U. Khan, S. Kumar, and S. B. Khan, "Handbook of materials characterization". Springer, 2018.

[52] A. Abdullah and A. Mohammed, ‘'Scanning electron microscopy (SEM): A Review’', Proc. 2018 Int. Conf. Hydraul. Pneum. - HERVEX, pp. 77–85, 2019.

[53] A. Dutta, "Fourier transform infrared spectroscopy'’, Spectrosc. methods Nanomater. Charact., pp. 73–93, 2017.

[54] T. K. Hamad, R. M. Yusop, W. A. Al-Taa’Y, B. Abdullah, and E. Yousif, ‘'Laser induced modification of the optical properties of nano-zno doped PVC films'’, Int. J. Polym. Sci., vol. 2014, doi: 10.1155/2014/787595, 2014.

[55] H. Singh, T. Singh, and J. Sharma, ‘'Review on optical, structural and electrical properties of ZnTe thin films: effect of deposition techniques, annealing and doping’', ISSS J. Micro Smart Syst., vol. 7, no. 2, pp. 123–143, doi: 10.1007/s41683-018-0026-2, 2018.

[56] T. Hamad, “Refractive index dispersion and analysis of the optical parameters of (PMMA/PVA) thin film”, J. Al-Nahrain Univ., vol. 16, no. 3, pp. 164–170, 2013.

[57] M. J. R. Aldhuhaibat, M. L. Hussein, M. T. Hyder, and M. S. Amana, '‘Study of the irradiation effect by -particles on optical properties of ZnO:6%In thin films'’, J. Phys. Conf. Ser., vol. 1484, no. 1, doi: 10.1088/1742-6596/1484/1/012003, 2020.

[58] W. D. Callister and D. G. Rethwisch, "Fundamentals of materials science and engineering", vol. 471660817. Wiley London, 2000.

[59] a M. Andriesh, M. S. Iovu, and S. D. Shutov, "Chalcogenide non-

crystalline semiconductors in optoelectronics'', J. Optoelectron. Adv. Mater., vol. 4, no. 3, pp. 631–647, 2002.

[60] H. S. Akbar, A. S. Jasim, and Z. S. Ali, "Effect of CO_2 Laser irradiation on the optical properties of cadmium oxide thin films grown by chemical spray pyrolysis (CSP) method'', IOSR J. Appl. Phys., vol. 08, no. 04, pp. 01–09, doi: 10.9790/4861-0804030109, 2016.

[61] N. Dhineshbabu, V. Rajendran, N. Nithyavathy,and, R. Vetumperumal, ''Study of structural and optical properties of cupric oxide nanoparticles'', Appl. Nanosci., vol. 6, no. 6, pp. 933–939, doi: 10.1007/s13204-015-0499-2, 2016.

[62] H. H. Issa, ''Effect of Tin content on structure , optical , electrical and photovoltaic effect of (Sb_2S_3) 1-x Sn x thin films'. Msc Thesis. Baghdad University. College of Science , 2014.

[63] R. M. Brza, B. Aziz, H. Anuar, F. Ali, E. Dannoun, S. Saeed, and, S. Mohammed, ''Green coordination chemistry as a novel approach to fabricate polymer:Cd(II)-complex composites: structural and optical properties'', Optical Materials: X, Elsevier B.V., pp. 1–35. doi: 10.1016/j.omx.2020.100067, 2020.

[64] M. A. Hussein , E. Dannoun , S. Aziz , M. Brza , R. Abdulwahid , S. Hussen , S. Rostam , and, D. Mustafa, ''Steps toward the band gap identification in polystyrene based solid polymer nanocomposites integrated with tin titanate nanoparticles'', Polymers (Basel)., vol. 12, no. 10, pp. 1–21, doi: 10.3390/polym12102320, 2020.

[65] B. H. Rabee and B. A. Al-Kareem, ''Study of optical properties of (PMMA-CuO) nanocomposites'', Int. J. Sci. Res, vol. 5, no. 4, 2016.

[66] T. S. Soliman and S. A. Vshivkov, ''Effect of Fe nanoparticles on the structure and optical properties of polyvinyl alcohol nanocomposite films'', J. Non. Cryst. Solids, vol. 519, no. May, doi: 10.1016/j.jnoncrysol.2019.05.028,2019.

[67] S. Yasmeen, F. Iqbal, T. Munawar, M. A. Nawaz, M. Asghar, and A. Hussain, ‘'Synthesis, structural and optical analysis of surfactant assisted ZnO–NiO nanocomposites prepared by homogeneous precipitation method'’, Ceram. Int., vol. 45, no. 14, pp. 17859–17873, doi: 10.1016/j.ceramint.2019.06.001, 2019.

[68] E. M. Khoder and J. S. Muhammad, '‘Effect of γ-radiation on optical properties of (PMMA : Blue Methyl) films'’, Diyala J. Pure Sci., vol. 11, no. 1, pp. 96–106, 2015.

[69] A. Hashim and Q. Hadi, ‘'Structural, electrical and optical properties of (biopolymer blend/titanium carbide) nanocomposites for low cost humidity sensors'’, J. Mater. Sci. Mater. Electron., vol. 29, no. 13, pp. 11598–11604, doi: 10.1007/s10854-018-9257-z, 2018.

[70] S. Anantha Ramakrishna, ‘'Physics of negative refractive index materials'’, Reports Prog. Phys., vol. 68, no. 2, pp. 449–521, doi: 10.1088/0034-4885/68/2/R06, 2005.

[71] I. S. Aziz , E. Dannoun, D. Tahir , S. Hussen, R. Abdulwahid, M. Nofal , R. Abdullah, and, A. Hussein, ‘Synthesis of PVA/CeO_2 based nanocomposites with tuned refractive index and reduced absorption edge: Structural and optical studies'’, Materials (Basel)., vol. 14, no. 6, pp. 2–19, doi: 10.3390/ma14061570, 2021.

[72] M. Rashidian and D. Dorranian, ‘'Low-intensity UV effects on optical constants of PMMA film’', J. Theor. Appl. Phys., vol. 8, no. 2, doi: 10.1007/s40094-014-0121-0, 2014.

[73] T. A. Taha, ‘'Optical properties of PVC/$A_{l2}O_3$ nanocomposite films'’, Polym. Bull., vol. 76, no. 2, pp. 903–918, doi: 10.1007/s00289-018-2417-8, 2019.

[74] C. Zilg, D. Kaempfer, R. Thomann, R. Mülhaupt, and G. C. Montanari, '‘Electrical properties of polymer nanocomposites based upon organophilic layered silicates'’, Conf. Electr. Insul. Dielectr. Phenom.

(CEIDP), Annu. Rep., pp. 546–550, doi: 10.1109/ceidp.2003.1254913, 2003.

[75] R. K. Goyal, S. D. Samant, A. K. Thakar, and A. Kadam, ‘'Electrical properties of polymer/expanded graphite nanocomposites with low percolation’', J. Phys. D. Appl. Phys., vol. 43, no. 36, doi: 10.1088/0022-3727/43/36/365404, 2010.

[76] H. P.Barber, S. Balasubramanian, Y. Anguchamy, S. Gong, A. Wibowo, H. Gao, and , H.Ploehn, "Polymer composite and nanocomposite dielectric materials for pulse power energy storage", vol. 2, no. 4. doi: 10.3390/ma2041697, 2009.

[77] R. A. Abed and M. A. Habeeb, ‘'Effect of chromium chloride (CrC_{l2}) on the electrical properties for (PVA-PVP-CrC_{l2}) films'’, vol. 3, no. 8, pp. 8–16, 2013.

[78] A. Hashim,N. Hamid and M. Abbas, ‘'Enhanced dielectric properties of polyvinyl alcohol doped with ZrC Nanoparticles’', World J. Adv. Res. Rev., vol. 15, no. 2, pp. 478–482, doi: 10.30574/wjarr.2022.15.2.0838, 2022.

[79] S. PRASHER, M. SINGH, and S. KUMAR, ‘'Analysis of electrical properties of Li 3 + ion beam irradiated iexan polycarbonate'’, vol. 21, no. 10, pp. 43–46, 2009.

[80] M. Musterman and P. Placeholder, ‘'About of The preparation and antibacterial activity cellulose / ZnO composite : a review ", Open Chem., vol. 12, no. 2, pp. 9–20, 2018.

[81] A. Azam, A. S. Ahmed, M. Oves, M. S. Khan, S. S. Habib, and A. Memic, ‘'Antimicrobial activity of metal oxide nanoparticles against Gram-positive and Gram-negative bacteria: A comparative study’', Int. J. Nanomedicine, vol. 7, pp. 6003–6009, , doi: 10.2147/IJN.S35347, 2012.

[82] S. Tang and J. Zheng, ‘'Antibacterial activity of silver nanoparticles:

structural effects'', Adv. Healthc. Mater., vol. 7, no. 13, pp. 1–10, doi: 10.1002/adhm.201701503, 2018.

[83] I. Akkurt, H. Akyildirim, B. Mavi, S. Kilincarslan, and C. Basyigit, ''Gamma-ray shielding properties of concrete including barite at different energies'', Prog. Nucl. Energy, vol. 52, no. 7, pp. 620–623, doi: 10.1016/j.pnucene.2010.04.006, 2010.

[84] A. Hashim, ''Recent review on poly-methyl methacrylate (PMMA)-polystyrene (PS) blend doped with nanoparticles for modern applications'', Res. J. Agric. Biol. Sci., no. December, pp. 2–9, doi: 10.22587/rjabs.2019.14.3.2, 2019.

[85] L. M. Chaudhari and R. Nathuram, ''Absorption coefficient of polymers (polyvinyl alcohol) by using gamma energy of 0.39 MeV'', Bulg. J. Phys, vol. 37, no. 1, pp. 232–240, 2010.

[86] Shivananda.C S, "Synthesis of silver nanoparticles using silk fibroin: characterization and potential antibacterial applications", Mangalore University. doi: 10.13140/RG.2.2.20649.62566, 2017.

[87] M. A. Mohamed, J. Jaafar, A. F. Ismail, M. H. D. Othman, and M. A. Rahman, "Fourier transform infrared (FTIR) spectroscopy" Elsevier B.V, doi: 10.1016/B978-0-444-63776-5.00001-2, 2017.

[88] N. Zeng, Jianye Chen, S. Lv, Chunli Qin, Kening Zhou, Qin Pu, Na Song, and X. Wang, ''Antimicrobial and anti-biofilm activity of Polygonum chinense L.aqueous extract against Staphylococcus aureus'', Sci. Rep., vol. 12, no. 1, pp. 1–12, doi: 10.1038/s41598-022-26399-1, 2022.

[89] A. Hammadi and M. Almousawi, ''Cloning of DNA: a review'', Sci. J. Med. Res., vol. 5, no. 20, pp. 130–134, doi: 10.37623/sjomr.v05i20.7, 2021.

[90] A. Hashim, A. J. Kadham Algidsawi, H. Ahmed, A. Hadi, and M. A. Habeeb, ''Structural, dielectric, and optical properties for

(PVA/PVP/CuO) nanocomposites for pressure sensors'', Nanosistemi, Nanomater. Nanotehnologii, vol. 19, no. 1, pp. 91–102, doi: 10.15407/nnn.19.01.091, 2021.

[91] E. Sheha, H. Khoder, T. S. Shanap, M. G. El-Shaarawy, and M. K. El Mansy, ''Structure, dielectric and optical properties of p-type (PVA/CuI) nanocomposite polymer electrolyte for photovoltaic cells'', Optik (Stuttg)., vol. 123, no. 13, pp. 1161–1166, doi: 10.1016/j.ijleo.2011.06.066, 2012.

[92] S. A. Khorrami, R. Islampour, H. Bakhtiari, and Q. S. M. Naeini, ''The effect of molar ratio on structural and magnetic properties of $BaFe_{12}O_{19}$ nanoparticles prepared by sol-gel auto-combustion method'', vol. 3, no. 3, pp. 191–197, 2013.

[93] K. Suresh, R. V. Kumar, and G. Pugazhenthi, ''Processing and characterization of polystyrene nanocomposites based on Co–Al layered double hydroxide'', J. Sci. Adv. Mater. Devices, vol. 1, no. 3, pp. 351–361, doi: 10.1016/j.jsamd.2016.07.007, 2016.

[94] C. Borsoi, L. C. Scienza, and A. J. Zattera, ''Characterization of composites based on recycled expanded polystyrene reinforced with curaua fibers'', J. Appl. Polym. Sci., vol. 128, no. 1, pp. 653–659, doi: 10.1002/app.38236, 2013.

[95] H. A. Ayesh, S. Ibrahim, A. Al-Jaafari, R. Abdel-Rahem, and , N.Sheikh, ''Electrical and mechanical properties of β-hydroxynaphthoic acid− multiwalled carbon nanotubes−polystyrene nanocomposites'', J. Thermoplast. Compos. Mater., vol. 28, no. 6, pp. 1–16, doi: 10.1177/0892705714533374, 2014.

[96] M. A. Arif, J. Yabagi, M.Hussin1, Yee See Khee, M. Kimpa, and, M. Muhammad, ''Synthesis and microwave absorption properties of doped expanded polystyrene with silver nanoparticles'', J. Sci. Technol., vol. 9, no. 3, pp. 33–40, 2017.

[97] E. Soleimani and M. Mohammadi, ''Synthesis, characterization and properties of polystyrene/NiO nanocomposites'', J. Mater. Sci. Mater. Electron., vol. 29, no. 11, pp. 9494–9508, doi: 10.1007/s10854-018-8983-6, 2018.

[98] M. H. Parangusan, D. Ponnamma, S. Adham and M.Hassan, ''Designing carbon nanotube-based oil absorbing membranes from gamma irradiated and electrospun polystyrene nanocomposites'', Materials (Basel)., vol. 12, no. 5, p. 709, doi: 10.3390/ma12050709, 2019.

[99] R. G. Kadhim, ''Study of some optical properties of polystyrene - copper nanocomposite films'', World Sci. News, vol. 30, pp. 14–25, 2016.

[100] F. T. Al-Hussein and B. H. Rabee, ''Optical properties of (PS-TiO_2-$A_{l2}O_3$) nanocomposite films injected with air nano bubbles'', NeuroQuantology, vol. 20, no. 3, pp. 01–07, doi: 10.14704/nq.2022.20.3.nq22032, 2022.

[101] W. A. Al-Taa'y, H. Ibraheem, E. Yousif, and H. Jelassi, ''Studies on surface morphology and electrical conductivity of PS thin films in presence of divalent complexes'', Baghdad Sci. J., vol. 16, no. 3, pp. 588–594, doi: 10.21123/bsj.2019.16.3.0588, 2019.

[102] H. Neama and N. Al-khegani, ''The eEffect of ferrous chloride ($FeC_{l\ 2}$) on some optical properties of polystyrene'', Acad. Res. Int., vol. 5, no. 2, pp. 161–166, 2014.

[103] A. G. Hadi, Z. Al-Ramadhan, and A. Hashim, ''Enhanced optical characteristics and low energy gap of $SrTiO_3$ doped polymeric blend for optoelectronics devices', J. Phys. Conf. Ser., vol. 1963, no. 1, doi: 10.1088/1742-6596/1963/1/012004, 2021.

[104] R. M. Mohammed, ''Effect of antimony oxide nanoparticles on structural, optical and AC electrical properties of (PEO-PVA) blend

for antibacterial applications'', Int. J. Emerg. Trends Eng. Res., vol. 8, no. 8, pp. 4726–4738, doi: 10.30534/ijeter/2020/107882020, 2020.

[105] A. Hashim, Y. Al-Khafaji, and A. Hadi, "Synthesis and characterization of flexible resistive humidity sensors based on PVA/PEO/CuO nanocomposites'', Trans. Electr. Electron. Mater., vol. 20, no. 6, pp. 530–536, doi: 10.1007/s42341-019-00145-3, 2019.

[106] S. Sabbah, M. Hasan, B. Yehiaa, and Z. Satar, ‘'The effect of metal powder on the optical properties of polyvinyl acetate'', J. Adv. Res. Appl. Sci., vol. 3, no. 1, pp. 1–6, doi: 10.53555/nnas.v3i1.666, 2016.

[107] A. K. and A. H. M.A.Habeeb, A.Hashim, ‘'Fabrication of (PVA-PAA) blend-extracts of plants Bio-composites and studying their structural, electrical and optical properties for humidity sensors applications'', Am. Sci. Publ., vol. 15, no. 7, pp. 589–596, doi: https://doi.org/10.1166/sl.2017.3856, 2017.

[108] O. K. Abdali and O. Abdulazeez, ''Optical and dielectrical properties of (PEG-CMC) films prepared by drop casting method'', World Sci. News, vol. 46, pp. 189–203, 2016.

[109] M. B. Mohamed and M. H. Abdel-Kader, ''Effect of annealed ZnS nanoparticles on the structural and optical properties of PVA polymer nanocomposite'', Mater. Chem. Phys., vol. 241, doi: 10.1016/j.matchemphys.2019.122285, 2020.

[110] A. F. Mansour, A. Elfalaky, and F. A. Maged, ‘'Synthesis, characterization and optical properties of PANI/ PVA blends'', IOSR J. Appl. Phys., vol. 7, no. 4, pp. 37–45, doi: 10.9790/4861-07433745, 2015.

[111] A. Hadi, A. Hashim, and Y. Al-Khafaji, ‘'Structural, optical and electrical properties of PVA/PEO/SnO_2 new nanocomposites for flexible devices'', Trans. Electr. Electron. Mater., vol. 21, no. 3, pp. 283–292, doi: 10.1007/s42341-020-00189-w, 2020.

[112] S. M. Hassan, ''Optical properties for prepared polyaniline / Ferro fluid nano composites'', Iraqi J. Phys., vol. 14, no. 31, pp. 161–168, doi: 10.30723/ijp.v14i31.183, 2019.

[113] M. A. Habeeb, A. Hashim, and B. H. Rabee, ''Study the electrical properties of PS-CaO composites'', Am. J. Sci. Res., no. 72, pp. 5–9, 2012.

[114] L. Abd El-Wahab and A. El-Hag Ali, ''Dielectric properties, Impedance analysis, and electrical conductivity of Ag doped radiation grafted polypropylene'', Egypt. J. Radiat. Sci. Appl., vol. 30, no. 1, pp. 95–107, doi: 10.21608/ejrsa.2017.1260, 2017.

[115] N. Mahfoudh, K. Karoui, and A. BenRhaiem, ''Optical studies and dielectric response of $[DMA]_2MC_{l4}$(M=Zn and Co) and $[DMA]_2ZnBr_4$'', RSC Adv., vol. 11, no. 40, pp. 24526–24535, doi: 10.1039/d1ra03652a, 2021.

[116] B. H. A. H. Rabee, ''Dielectric properties of PS-$BaSO_4$. $5H_2O$ composites'', Eur. J. Soc. Sci., vol. 32, no. 1450–2267, pp. 316–320, 2012.

[117] D. Hassan and A. H. Ah-Yasari, ''Fabrication and studying the dielectric properties of (Polystyrene-copper oxide) nanocomposites for piezoelectric application'', Bull. Electr. Eng. Informatics, vol. 8, no. 1, pp. 52–57, doi: 10.11591/eei.v8i1.1019, 2019.

[118] A. Hashim and Z. S. Hamad, ''Antibacterial activity of biopolymer blend- carbide nanoparticles Bio-films against escherichia coli'', Res. J. Agric. Biol. Sci., vol. 13, no. 2, pp. 1–5, doi: 10.22587/rjabs.2018.13.2.1, 2018.

[119] A. Hashim, I. R. Agool, K. J. Kadhim, and A. Hashim, ''Novel of (polymer blend-Fe_3O_4) magnetic nanocomposites : preparation and characterization for thermal energy storage and release , gamma ray shielding , antibacterial activity and humidity sensors applications'', J.

Mater. Sci. Mater. Electron., vol. 29, no. 12, pp. 10369–10394, doi: 10.1007/s10854-018-9095-z, 2018.

الخلاصة

حضرت المتراكبات النانوية (للبولي ستايرين/اوكسيد السليكون / أوكسيد تيتانات السترونتيوم) بطريقة محلول الصب بتراكيز مختلفة من جسيمات اوكسيد السليكون و أوكسيد تيتانات السترونتيوم النانوية لدراسة الخصائص البصرية والتركيبية وكذلك الكهربائية للمتراكبات النانوية. لاستخدامها في النشاط المضاد للبكتيريا وتطبيق أشعة كاما. ان الخصائص التركيبية تشمل كل من المجهر الضوئي (OM) ، ومجهر الإلكتروني (SEM) ، وتحويلات فوريه (FTIR)اظهرت صور المجهر الضوئي عن توزيع متجانس للجسيمات النانوية وتشكيل مسارات شبكية داخل المصفوفة البوليمرية بزيادة تراكيز للجسيمات النانوية. أظهرت صور SEM توزيعًا متجانسًا وجيدًا في مورفولوجيا السطح. تشير نتائج قياسات FTIR إلى وجود تراكب فيزيائي بين البوليمر والجسيمات النانوية. أظهرت نتائج الخواص البصرية للمتراكبات النانوية (PS / SiO_2- $SrTiO_3$) الى زيادة الامتصاصية و معامل الامتصاص ومعامل الخمود وثابت العزل الكهربائي الحقيقي والخيالي والموصلية البصرية ومعامل الانكسار مع زيادة تراكيز الجسيمات النانوية بينما تنخفض فجوة الطاقة والنفاذية. أظهرت نتائج الخواص الكهربائية للمركبات النانوية أن ثابت العزل و فقد العازل الكهربائي للمتركبات النانوية انخفض مع زيادة تردد المجال الكهربائي في نفس الوقت تزداد التوصيلية الكهربائية للتيار المتناوب. بزيادة تركيز الجسيمات النانوية (SiO_2- $SrTiO_3$) يؤدي إلى زيادة التوصيلية الكهربائية للتيار المتناوب والعزل الكهربائي وكذلك يزداد فقد العازل الكهربائي . أظهرت نتائج تطبيق مضادات البكتيريا للمتراكبات النانوية (PS / SiO_2-$SrTiO_3$) أن منطقة التثبيط لـــ (E. coli) و (S. aureus) تزداد بزيادة تراكيز الجسيمات النانوية (SiO_2- $SrTiO_3$). ان نتائج تطبيقات أشعة كاما تبين عندما تزداد الجسيمات النانوية (SiO_2- $SrTiO_3$) سوف تزداد معاملات التوهين الخطي لأشعة كاما.

جمهورية العراق
وزارة التعليم العالي والبحث العلمي
جامعة بابل
كلية التربية للعلوم الصرفة
قسم الفيزياء

تحسين بعض الخصائص الفيزيائية لـ PS/SiO_2- $SrTiO_3$ للتطبيقات البيئية

رسالة مقدمة

إلى مجلس كلية التربية للعلوم الصرفة في جامعة بابل وهي جزء من متطلبات درجة الماجستير في التربية\ الفيزياء

من قبل الطالب

أرشد فاضل كاظم مطرود

بكالوريوس تربية فيزياء 2011

بأشراف

أ.د. احمد هاشم محيسن

2023م 1444هـ